VIDEO STREAMING OVER COGNITIVE RADIO NETWORKS

by

Maram Wahed R. Helmy

A Thesis Presented to the Faculty of the
American University of Sharjah
College of Engineering
in Partial Fulfillment
of the Requirements
for the Degree of

Master of Science in
Electrical Engineering

Sharjah, United Arab Emirates

July 2020

Declaration of Authorship

I declare that this thesis is my own work and, to the best of my knowledge and belief, it does not contain material published or written by a third party, except where permission has been obtained and/or appropriately cited through full and accurate referencing.

Maram Wahed R. Helmy

08/06/2020

Approval Signatures

We, the undersigned, approve the Master's Thesis of Maram Wahed R. Helmy

Thesis Title: Video Streaming over Cognitive Radio Networks

Date of Defense: 29/07/2020

Name, Title and Affiliation	**Signature**
Dr. Mohamed S. Hassan Professor, Department of Electrical Engineering Thesis Advisor	
Dr. Mahmoud H. Ismail Ibrahim Associate Professor, Department of Electrical Engineering Thesis Co-Advisor	
Dr. Hassan Mir Associate Professor, Department of Electrical Engineering Thesis Committee Member	
Dr. Yasmin Aly Hassan Fahmy Professor, Department of Electronics and Communication University of Cairo Thesis Committee Member	
Dr. Nasser Qaddoumi Head, Department of Electrical Engineering	
Dr. Lotfi Romdhane Associate Dean for Graduate Studies and Research, College of Engineering	
Dr. Sirin Tekinay Dean College of Engineering	
Dr. Mohamed El-Tarhuni Vice Provost for Graduate Studies Office of Graduate Studies	

Acknowledgements

I would like to thank Allah for His blessings and for giving me the strength to complete my degree.

I would like to express my sincere gratitude and thanks to my research advisors; Dr. Mohamed S. Hassan and Dr. Mahmoud H. Ismail, who provided valuable feedback, continuous support and guidance throughout the research process. Many thanks also to committee members for their valuable comments and feedback, and to my family and my supportive husband for their encouragement which helped me in completion of this work.

I would like to extend my special thanks to Prof. Nasser Qaddoumi, the Head of Electrical Department at AUS for all of his continuous support, and for all the professors in the Electrical Engineering Department who taught me and shared their valuable knowledge. Finally, I want to thank the American University of Sharjah and the Department of Electrical Engineering for granting me Graduate Teaching Assistantship (GTA) to continue my studies.

Dedication

To

My parents for their love and support

My beloved husband for his encouragement

My beloved coming baby . . .

Abstract

The exponential increase in the demand for streaming video in wireless communication is obstructed by the problem of spectrum scarcity. In an effort to mitigate this problem, cognitive radio (CR) technology was proposed as a solution since it offers a great advantage to unlicensed users, also known as secondary users (SUs), by allowing them to opportunistically access the licensed primary bands. However, it is more challenging to deliver video services over CR networks not only because of the intermittent availability of the PU channels but also due to the challenges stemming from wireless channels and the quality requirements of the videos. In this work, several frameworks are proposed to stream scalable video sequences from a base station to multiple SUs over CR networks. One approach is a moments matching-based approach that enabled us to quantify the total amount of data that can be provided by the available PU channels. Specifically, a closed-from approximation for the distribution of the total amount of data available for SU over all the available PU channels during any arbitrary interval of time was obtained. The correctness of the obtained closed-form approximation is verified using simulations and numerical investigations. Another approach is employing the CR network over long-term evolution (LTE) standard platform. The objective of this work is to guarantee continuous playback at the SUs end with acceptable perceptual quality. To achieve this objective, different resource allocation schemes are introduced to adaptively assign the available radio channels to SUs while taking into considerations the quality of their assigned channels as well as their buffer occupancies. In addition, a streaming algorithm is introduced to guarantee the delivery of scalable video frames, with base and enhancement layers, within the delay constraints with priority given to the base-layer frames to guarantee the continuity of video playback. Furthermore, adaptive modulation is used based on the channel state information (CSI) as fed-back by SUs. The performance of the proposed schemes is evaluated through extensive evaluation and Monte-Carlo simulations in Matlab.

Search Terms: ***Cognitive radio networks, video streaming, Markov chain, method of moment, dynamic resource allocation, CRN over LTE, scalable vidoe coding***

Table of Contents

List of Figures

Chapter 1: Introduction

In this chapter we briefly introduced cognitive radio network along with the motivation of this work. Then, the problem addressed in this work and our contribution are described. The organization of this thesis is given at the end of this chapter.

1.1. Overview

Over the past few years, the demand for bandwidth-hungry applications (e.g. Netflix, Youtube, etc.,) has been exponentially growing. These applications have generated the majority of wireless and wired networks' traffic in the last decade, it is anticipated by Cisco that 82% of all IP traffic (both business and consumer) will be video traffic by 2020 [3]. Therefore, despite the recent advances in the wireless technology, multimedia applications will continue their increase in the demand for more bandwidth. As a result, the expected growth in wireless multimedia applications will always be challenged by their stringent quality-of-service (QoS) requirements in addition to the expected shortage of the radio spectrum, also known as the spectrum scarcity problem and caused by the static assignment of the licensed spectrum. According to [4], spectrum scarcity is not mainly due to shortage in the availability of the resources, but due to how they are licensed and how they are utilized. Recent measurements have shown that generally less than 5% of the statistically assigned spectrum is efficiently used [5]. Consequently, it was proposed to improve the spectrum utilization by allowing unlicensed users, known as secondary users (SUs) to opportunistically access the licensed bands of the licensed users, also known as primary users (PUs) [4]. Opportunistic dynamic spectrum access (DSA) is a paradigm that was first introduced in [6]. In DSA, the licensed radio spectrum is made accessible to SUs, when the PUs are idle. The absence of a PU from a specific frequency band at different points in time and space is called spectrum hole [7], which is a reserved portion of the spectrum that is not in use. Cognitive radio (CR) technology is a DSA technique that is expected to help to overcome the expected scarcity problem by efficiently utilizing the spectrum and hence pervasively meet the increasing demand for new wireless services. This inspired many researchers to study different schemes with which the inefficiently utilized spectrum can be dynamically allocated to SUs. Therefore, Cognitive Radio Networks (CRNs) were introduced as a promising solution for an efficient spectrum utilization by enabling interactive wireless users to sense and learn the surrounding environment and correspondingly adapt their transmission strategies [8].

1.2. Motivation and Thesis Objectives

Driven by the developing interest in streaming videos over wireless networks, and the advantages that CR networks can offer, we will focus on the problem of resource management and allocation of the inefficiently utilized spectrum to enable SUs to opportunistically access the PU channels. The objective of this work is moving toward two parallel directions. Firstly, to quantify the total amount of data that can be provided by the available PU channels using moment method. Secondly, to employ an LTE-based CR network. In the second direction, different resource allocation schemes are proposed to efficiently allocate the available resources among SUs. Our framework satisfied the SUs' requirements including fairness, the stringent quality requirements of the video applications, and provisioned quality of experience (QoE).

1.3. Research Contribution

We study and solve the problem of quantifying the total amount of data that can be provided by the available PU channels, how to allocate those available channels to SUs, and how to stream scalable video coding over CR networks.

- We propose a closed-from approximation for the distribution of the total amount of data available for SUs over all the available primary channels during any arbitrary interval of time.
- We propose an infrastructure LTE-based CR network that operates on LTE platform.
- We propose a dynamic resource allocation algorithms that adaptively assign the available channels to SUs based on their updated feedback information (SNR and buffer state) to avoid buffer starvation and guarantee continuous playback at the SUs end.

- We Propose a streaming algorithm that take the advantages of Scalable Video Coding (SVC) techniques to schedule video frames from different codded layers on the allocated channels for receiving the delivered frames correctly by their deadlines, and hence improve QoE.

1.4. Thesis Organization

The organization of this thesis is: Chapter 2 provides a background about CR network technology, recent resource allocation techniques, overview of LTE technology, SVC video coding. Moreover, related works in the literature are presented. Chapter 3 discusses the proposed probabilistic expression for the amount of data provided to SUs in CR networks. Chapter 4 discusses the proposed LTE-based CR network, the proposed dynamic allocation and streaming algorithms, and simulation results. Finally, conclusion is discussed in Chapter 5.

Chapter 2: Literature Review and Related Work

In this chapter, we briefly introduce the fundamentals of cognitive radio networks along with its architecture components, its challenges, and the advantages of applying this technology in video streaming applications. Then, recent techniques in the literature for resource allocation in CR networks are discussed. After that, a brief review about scalable video encoding technique is presented. Finally, the motivation of this work is introduced.

2.1. Cognitive Radio Networks: Definition, Architecture, and Challenges

The current spectrum allocation policy grants a fixed spectrum bands to licensed users for exclusive access for a long-term over large geographic areas [9]. While this policy has worked well in the past decades, recently, its drawbacks started to reveal. Such allocation policies have caused what is known today by spectrum scarcity. Recent measurements have reported that generally less than 5% of static licensed spectrum are used at any given time and location [5]. According to [4], the spectrum scarcity is not due to the availability of the resources, but how they are utilized. Consequently, new allocation policies were needed, and [4] proposed to improve the spectrum utilization by efficiently allowing unlicensed users, also known as secondary users (SUs), to opportunistically access the licensed primary bands of PUs. This inspired many researchers to study different schemes with which the inefficiently utilizing spectrum can be allocated to secondary users. Therefore, CR Networks were introduced as a promising solution for an efficient spectrum utilization by enabling interactive wireless users to sense and learn the surrounding environment and correspondingly adapt their transmission strategies [8].

2.1.1. CR networks architecture. Figure 1 [1] shows the components of a CR network architecture, which can be classified as primary and secondary network. The primary network is known as the legacy network in which the users have an exclusive right to access their licensed spectrum bands. Conversely, users in the cognitive network don't need a license to operate in the desired band. The basic components of the CR network are defined as follows [1]:

- Primary Users: Users with prerogative right to operate in a certain spectrum band. This access is only controlled by their base-station and operations of any other unlicensed user should not affect it.
- Primary Base-Station: It is a fixed infrastructure network component which has a spectrum license. It does not have any cognitive radio capability, however, it may be required to have both legacy and cognitive radio protocols for the primary network access of SUs.
- Secondary User: Users with no spectrum license. They are only allowed to opportunistically access the licensed band. SUs should be capable of spectrum sensing, spectrum decision, spectrum handoff and cognitive radio MAC/routing/transport protocols. In addition, they should be able to communicate with other SUs.
- Secondary Base-Station: It is a fixed infrastructure component with cognitive radio capabilities. It provides single hop connection to SUs without spectrum access license.

2.1.2. CR network challenges. Generally, there are four main challenges arise in CR networks. These challenges are spectrum sensing, spectrum decision, spectrum

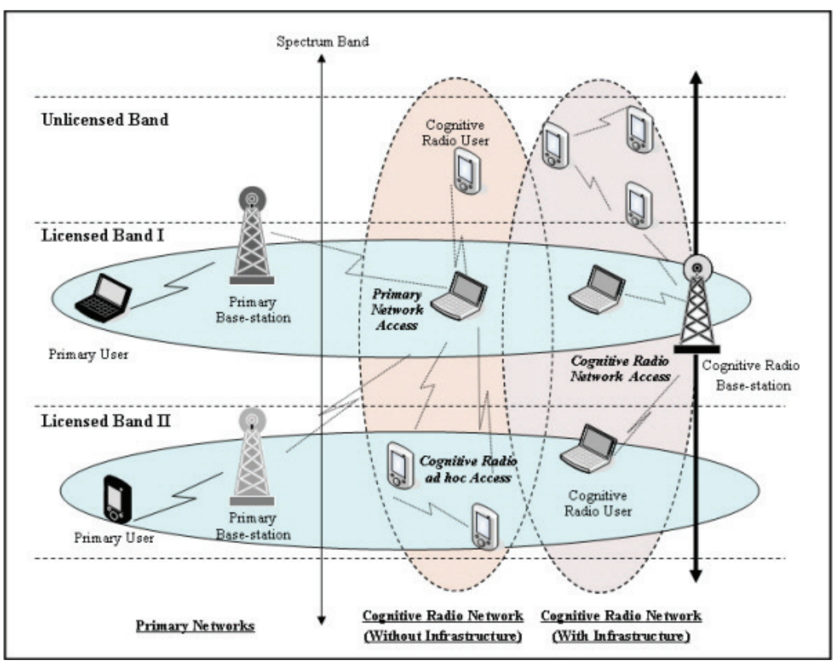

Figure 1: CR network architecture [1].

handoff, and spectrum mobility. Each challenge will be discussed in the next subsections.

- Spectrum sensing: Users with prerogative right to operate in a certain spectrum band. This access is only controlled by their base-station and operations of any other unlicensed user should not affect it.
- Primary Base-Station: It is a fixed infrastructure network component which has a spectrum license. It does not have any cognitive radio capability, however, it may be required to have both legacy and cognitive radio protocols for the primary network access of SUs.
- Secondary User: Users with no spectrum license. They are only allowed to opportunistically access the licensed band. SUs should be capable of spectrum sensing, spectrum decision, spectrum handoff and cognitive radio MAC/routing/transport protocols. In addition, they should be able to communicate with other SUs.
- Secondary Base-Station: It is a fixed infrastructure component with cognitive radio capabilities. It provides single hop connection to SUs without spectrum access license.

2.1.2.1. Spectrum sensing. Spectrum sensing plays a crucial role in deploying an effectual CR network. A SU should monitor the PU's activity pattern to detect spectrum holes before any transmission. While, during transmission a continuous sensing should be maintained to detect if any PU is accessing the band [10].

Several spectrum techniques were proposed in the literature. Most of these techniques can be categorized into three classes: non-cooperative detection, co-operative detection, and interference detection.

- Non-cooperative detection: It is the most basic technique where each SU independently senses the surrounding spectrum environment and then selects the best suitable spectrum band based on his own measurements. Such detection is formulated using hypothesis testing, where null hypothesis implies the absence of PU and the alternate hypothesis implies its presence [11]. One way is an energy detection based, where a SU measures the average energy in a certain band and compares it to a predefined threshold [12]. This technique has low computation complexity and can be easily implemented. A second approach is the matched filter detection where a prior information about the PU's signals such as the modulation type and order, pulse shaping, and the packet format is required [13]. Other approaches such as cyclostationary feature detection [14–17] and eigenvalue based detection are also used [18] [19]. In general, the non-cooperative detection technique is inconvenient as it requires high reception sensitivity so a SU can be able to differentiate and detect the PU's signals from noise signals.

- Cooperative detection: Non-cooperative spectrum sensing approaches are insufficient to provide accurate detection due to the effect of fading, shadowing, and other issues of wireless channels. Thus, cooperative sensing was proposed to improve the detection accuracy through cooperation among SUs. This technique is implemented in a decentralized mode or centralized mode. In the decentralized mode, SUs exchange the results of the individual sensing with each other, and then each SU takes its own decision. While, in the centralized mode a central node such as a base station is used to collect the sensing results from all SUs, then take the decision of spectrum band accessibility [9].
- Interference-based detection: this technique is based on identifying the presence and the position of PUs through the measurement of Interference Temperature (IT) [20]. By using this technique, PUs and SUs can simultaneously transmit as long as the interference from SUs is beyond the IT of PUs. However, there are many practical issues related with this technique.

2.1.2.2. Spectrum decision. After the spectrum is being sensed and the available bands are detected, then a SU can allocate a channel. Channel allocation is not a straightforward procedure as it involves internal and external polices. Wrong decisions might cause a large degradation in the performance of SUs. Hence, efficient resource management and allocation schemes have great impact on the performance of CR networks.

2.1.2.3. Spectrum sharing. In general, any CR network will have multiple SUs who are trying to access the available spectrum, thus there should be a coordination policy to avoid collision between them in the overlapping portion of the spectrum.

2.1.2.4. Spectrum mobility. SUs should immediately evacuate the portion of the spectrum in use if it is required by a PU. This might cause a large degradation in the performance of SUs. Thus, CR network should be capable of transferring the ongoing communication to another unused portion of the spectrum.

2.2. Resource Allocation Techniques

Resource allocation is a key mechanism that determines an optimal assignment of available resources among different SUs such that the performance of CR network is optimized based on some criteria such as maximize throughput, fairness, spectral efficiency [21]. However, the most basic requirement of a CR network is that SUs should not cause any interference to PUs. The most common techniques that are used in literature for resource allocation in CR networks are presented.

2.2.1. Heuristics based. Finding an optimal solution for the resource allocation problem is highly complex. According to [22] the channel assignment problem is an NP-complete problem, thus there is no known way to find a solution quickly. To overcome this issue, heuristic techniques are often used to find near-optimal solution at reasonable computational cost for algorithmically complex and time-consuming problems [21]. There is no a specific algorithm solution for resource allocation problem in CR network. Most of the approaches in the literature are problem-specific as in [23–25]. Heuristic techniques are iterative algorithm, which finds at each iteration the best local solution, which can be, in the resource allocation context, the SU with the highest priority for accessing the spectrum, the channel with highest SINR or lowest traffic, etc.

For example, in [24] they proposed a heuristic channel allocation to lower the complexity of the optimization problem they obtained, which is in $O(n^3)$, where n is the number of the active SUs in the network. The proposed algorithm randomly selects a PU and a SU at each iteration. During each iteration, the selected SU scans the selected primary channel to gather information about the transmission power of the PU and channel status. By assuming that PUs are less than SUs, after some iterations all the primary channels will be scanned and SUs can select their channels.

In [26], the resource allocation problem was expressed as an Integer Linear Programming (ILP) problem and a heuristic scheme was proposed. The idea of the scheme is to divide the available bands into M sets and each SU_i forms a preferable channel list for the other SUs. Based on the distance from the $i-th$ user and the SINR of the channel, the channels with lower SINR will be assigned to the closest users.

Heuristic techniques are simple and can be easily implemented to find near-optimal solutions [27], however, the solutions are problem-dependent, there is no analytical methodology to study their convergence, and they can get stuck in local optimal solution, which can be far from global optimal solution.

2.2.2. Game theory based. Game theory is a mathematical framework that is extensively used in the literature to model the cooperation and conflict between rational users. The concept of game theory fits well with the resource allocation problem as the action of one player (SU) directly affects the action of others. [28–30] used game theory to solve the resource allocation problem to find the optimal solution through the Nash equilibrium. The resource allocation can be formulated as a set of players (SUs) who are competing for the set of the available primary channels in order to maximize their utility function and meet their requirements. The utility function may account for selfish users (evaluating each channel based on the level of interference observed by that particular channel), cooperative users (by taking into account the interference to neighbors SUs as well) [29], fairness among users [31], minimize spectrum hand-off [32], etc.

Generally, the game theory model is a powerful decision making framework that can be applied in cooperative and non-cooperative SUs, however, the game formulation and utility function must be very well structured to guarantee equilibrium.

2.2.3. Linear programming based. Another technique that is used in the literature to solve the resource allocation problem is the Linear programming method [33–35]. LP is a technique for optimizing a linear objective function subject to linear constrains. Resource allocation problem can be formulated as a Mixed Integer Non-Linear Programming (MINLP) problem. The MINLP problem can be translated into a Binary Linear Program (BLP) that contains only binary parameters and linear objective function with linear constrains. Such transformation is applied to simplify the MINLP problem to BLP problem that can be solved using standard linear programming (LP) techniques. However, transforming MINLP into BLP is not guaranteed and requires several assumptions [21].

2.2.4. Fuzzy logic based. Fuzzy logic is a used technique for decision making and optimization algorithms in resource allocation [36, 37]. A fuzzy logic controller (FLC) is composed of four modules: a fuzzy rule base (a set of rules in the form of ”IF-THEN”), a fuzzy inference engine, a fuzzification and defuzzification module.

The input of the FLC can be the arrival rate of PUs or SUs, the channel availability, the distance between users, the velocity (if SUs are moving), etc [21]. Then, the controller takes a decision based on predefined rules on which SU will select which available band. This technique can be only used when the configuration of the CR network is known a prior. The disadvantages of FLC are its limited functionality as it requires pre-defined rules and the large number of rules that need to be considered for the dynamic nature CR networks.

2.2.5. Evolutionary algorithms based. Evolutionary algorithms (EAs) are stochastic search techniques that mimic evolution and social behavior. The most popular type of EA is Genetic Algorithms (GAs). In [38–42] they used genetic algorithms to find optimum solution for resource allocation in CR network. GAs are different from other algorithms that they reflect the process of natural selection where the fittest individuals are selected for reproduction in order to produce offspring of the next generation. The process begin with a set of individuals, called population, where each individual is a solution of the optimization problem that is characterized by a set of parameters to form chromosomes. Chromosomes usually specify a possible conflict free channel assignment matrix, that is encoded in a way to avoid redundancy of elements. To evaluate the fitness of the chromosome, it should be mapped to the channel assignment matrix [21].

Another approach that is used is swarm intelligence. [43] proposed the following model: the probability of a successful transmission of a user is broadcasted and used as a pheromone, where SUs received the broadcast massage and adjust their parameter accordingly. If the channel transmission probability decreases, then SUs wil have lower probability of accessing it.

Another algorithm that is used in the literature is the Artificial Bee Colony (ABC) that is inspired by honey bee foraging. The ABC algorithm consists of three groups of bees: employed bees, onlookers and scouts. The number of employed bees in the colony are equal to the number of food resources. Onlookers explore and share the information of food resources. Scouts search for new food sources after abandoning their own. The possible solutions are introduced by the location of the employed bees, while the quality of the solution is represented by the amount of nectar of the source. In resource allocation context, the location of one onlooker represents a possible channel assignment, while the amount of nectar is the maximized utility function [44].

2.3. Overview of LTE Network

Long-Term Evolution (LTE) is a network technology which was developed by the 3rd Generation Partnership Project (3GPP) to provide high data rate, low latency and support flexible bandwidth [2]. LTE applies Orthogonal Frequency Division Multiplexing (OFDM) which allocates multiple resource blocks of 180 kHz each to each user [45]. LTE bandwidth ranges from 5 MHz to 20 MHz. It supports both Time Division Duplexing (TDD) and Frequency Division Duplexing (FDD). The eNodeB is the part that is responsible for resource allocation based on network configuration, network load and user requests. [46]. LTE Downlink (DL) adopts Orthogonal Frequency Division Multiple Access (OFDMA) and the resources are specified in frequency and time domain [46]. The resource element is defined as the smallest resource unit with a duration of 66.667 microseconds which represents one symbol. Resources are assigned to a user in term of Resource Block (RB). One resource block groups seven consecutive symbols and occupies one time slot with a duration of 0.50 ms. Every two time slots form a sub-frame with a duration of 1 ms and 10 sub-frames represent one frame with a period of 10 ms. The eNodeB performs scheduling every 1 ms Transmit Time Interval (TTI) [45]. Figure 2 illustrates the structure of the LTE resource grid in the time and frequency domains.

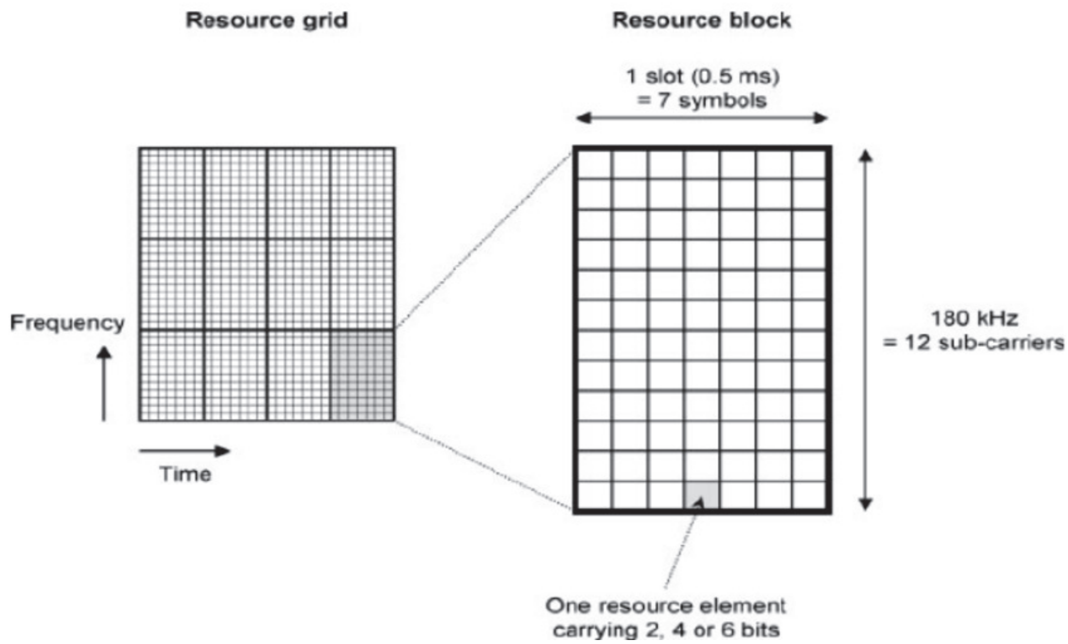

Figure 2: Structure of the LTE resource grid in the time and frequency domains [2].

2.4. Overview of Video Structure

Video is a sequence of images (frames) displayed in a sequence order. Three types of frames (pictures) are used in video compression

- Intra-Coded picture (I frame): contain an entire image and coded independently without reference to any other frame except themselves.
- Predicted picture (P frame): coded relative to the content of the preceding frame either P or I. It holds only the changes in the image from the previous frame.
- Bi-directional predicted picture (B frame): coded with the reference to previous and future frame either I or P. Group of Pictures (GOP) defines how the order of I, P, and B frames are arranged.

2.4.1. Scalable video coding. Video streaming has become the dominant traffic in wireless network. The bandwidth-hungry nature of multimedia applications allows it to become one of the candidates that are going to fully benefit from the potential of CR networks. The main challenge of streaming a video over a CR network is to maintain stable and optimal video quality under the time-varying nature of a wireless channel. To overcome this challenge, the idea of layered video coding was introduced.

Scalable Video Coding (SVC) is a standard technique for video compression that allows encoding a video stream into multiple layers; the base layer (BL) which contains the essential bits required to decode the video sequence at an acceptable quality level, and the enchantment layer(s) (EL) which contains bits that are used to improve stream quality. However, the ELs can't be decoded without receiving the BLs. SVC works as a source control mechanism , where source rate is adopted according to the variations of channel bandwidth to guarantee continuous playback and avoid buffer starvation which results in degradation in quality of the received video [47]. By applying SVC, the video is encoded once and it can be decoded in different ways depending on the network conditions and user capabilities (i.e CPU capabilities and bandwidth). Recently, different scalable video coding (SVC)techniques have been studied and proposed to support heterogeneous networks with diverse users.

Scalable video coders are of different implementations, this includes coarse-grained scalable (CGS), medium grained scalable (MGS) and fine-grained scalable (FGS). H.264/SVC is the standard for scalable video coding [48]. SVC supports three types of scalability, temporal, spatial and quality SNR scalability. First, temporal scalability refers to the extraction of the video content at different temporal resolutions (frame rate). Second, spatial scalability allows incorporating multiple spatial resolutions (e.g., HD, SD) of the same video in a single bit stream. Finally, quality scalability (or SNR scalability) refers to the possibility of extracting different quality variations of the same video from a single bit stream trading off visual distortion [49].

Recently, researchers have been interested to take the advantages offered by CR networks to stream multimedia survives. In multimedia services, the Quality of Service (QoS) at the application layer is the most important factor from user's prospective. Some of the works that have been done in CR networks focused on maximizing the throughput of SUs. However, other studies have showed that maximizing the throughput dose not necessarily guarantee maintaining the required QoS at the application layer [50].

The work in [8] focused on delay-sensitivity multimedia applications and consider a scenario where SUs share a single-hop wireless adhoc network. A priority virtual queue interface was proposed for heterogeneous multimedia users. In this scheme, the SUs exchange their information and time share the various frequency channels in a decentralized fashion. A dynamic learning algorithm is then developed based on the priority queue analysis which assists the SUs to track the actions of the other users and adequately adapt their own strategies and actions.

2.5. Related Works

2.5.1. Multimedia services over CR networks. In [51–53], they focused on streaming scalable encoded video-on-demand over CR networks. They consider an infrastructure-based CR system. They proposed a channel allocation scheme that jointly consider the status of the playback buffers at the SUs and the quality of the available channels while allocating channels among active SUs. They also proposed a streaming algorithm that schedules the video frames by taking the benefit of SVC and the adaption of the used modulation level on the channel conditions to meet a predetermined target bit error rate (BER).

In [54], they proposes an opportunistic switching-based and delay-aware scheduler that maximizes the total throughput for centralized CRNs. The scheduler is an inter-frame scheduler that helps in reducing the effect of hardware switching delay by excuting the scheduling and allocation for multiple consecutive time slots. The proposed scheduler jointly considers the delay associated with the scheduling process as well as the effect of spectrum switching delay. They formulated an optimization problem to find the optimum scheduler while taking into account the switching delay, the PU activity, historical information on the PU behavior, the channel quality, and the status of the SUs.

In [55], they proposed a novel low complexity stochastic based rate control approach for streaming SVC video sequences. The approach is applied by obtaining an exact closed-form expression for the statistical distribution of the total amount of data that can be transmitted over the available PU channels for any arbitrary interval of time. Then, thr rate control mechanism was devised to fit SUs' data in the available data budget. A comprehensive study was conducted to study the effect of the proposed rate control scheme on the continuity and quality of the reconstructed video sequences.

In [56] , they proposed a content driven proportionate channel allocation scheme for streaming SVC over CR network. The proposed allocation scheme takes into consideration the various requirements of secondary applications while maintaining the long term fairness among SUs. The main aim of the work was to improve the overall satisfaction of the SUs (QoE) especially for rapid motion (RM) type of video users.

In [57], they investigated the problem of multicast multimedia streaming in multi-hop CR networks. They proposed an intelligent multicast routing protocol for multi-hop ad hoc CRNs that can supports multimedia streaming. The proposed protocol performs path selection and channel assignment phases for the different multi-cast receivers. Path selection is based on the shortest path tree (SPT) that performs the expected transmission count metric (ETX). While, channel selection is based on the ETX, which is a function of the probability of success (POS) over the different channels that depends on the channel-quality and availability.

In [58], they focused on multimedia transmissions over multi-hop CR networks. They proposed a cross layer routing scheme for transmitting adaptive bitrate video where the best path is chosen based on the value of end-to-end path stability time and end-to-end path delay along with the real time multimedia QoS requirements. Also, they introduced a periodic path updation scheme to guarantee path continuity, avoid the interference with the PU, improve the channel utilization and error resilience.

The work in [59] addresses the problem of estimating and/or identifying the achievable quality of service (QoS)-levels over the available licensed channels. They proposed a novel channel quantification and QoS-levels identification scheme which is known as NOn-parametric Bayesian channEls cLustering (NOBEL). The proposed scheme exploits the PUs' channel usage features and models them by using an infinite Gaussian mixture model and collapsed Gibbs sampling model. The proposed scheme assists SUs to find an appropriate channel to meet the requirements of their multimedia application.

2.5.2. LTE-based CR network. CR networks are considered to be the future of the cellular networks in the context of spectrum sharing between different operators. Spectrum sharing allows lightly loaded operator to share their unused spectrum with another operator to efficiently utilize the spectrum. This is relevant in the context of the 4G cellular standard 3GPP LTE-A due to the recently introduced carrier aggregation (CA) feature [60, 61]. LTE is chosen as the implementation platform of CR networks due to its desirable characteristics, such as spectrum flexibility, fast adaptation to time-varying channel conditions, high spectral efficiency and robustness against interference [62, 63].

Authors in [60] presented a case of sensing for dynamic spectrum sharing in Cognitive LTE-A cellular networks. They developed and analyzed energy detectors that is designed to solve the problem of sensing in presence of a desired signal in presence of a desired signal in the context of an LTE-A based system.

The target of the work done in [64] was to implement a spatial interweave LTE-TDD based cognitive radio. They argued that using LTE as the physical layer of the CR network would results in a high spectral efficiency network. They focused on spatial interweave CR network in which a SU uses an antenna array to perform null-beamforming in the PU's direction in order to spatially reuse the spectrum. They proposed innovative solutions to avoid interference to the primary system where they designed at the secondary base station an over-the-air calibration technique and a beamforming strategy based on the channel reciprocity hypothesis inherent in TDD systems.

Authors in [65] proposed a coordinated dynamic spectrum access scheme for LTE based on cognitive radio (CR) technology ,where a central entity and Spectrum Policy Server (SPS) is responsible for spectrum management in a LTE multi operator heterogeneous network (HetNet). They found that their proposed architecture improved spectral efficiency and enhanced data rates.

Authors in [63] studied the problem of transmission power and bandwidth allocation in a cognitive LTE based network consisting of secondary eNBs with different requirements on SINR and application-layer QoS. They proposed a novel resource allocation strategy in which the total queue size in enhanced NodeBs (eNBs, primary and secondary) is minimized subject to interference requirements and queue stability constraints of the primary eNBs. Their proposed algorithm showed low complexity and outperformed previously proposed schemes.

Chapter 3: A Probabilistic Expression for the Amount of Data Provided to Cognitive Users in CR Networks

In this chapter, we formulate the problem of quantifying the total amount of data that can be provided by the available PU channels using moment method.

3.1. Problem Formulation

The problem we investigate in this chapter is to quantify the total amount of data that can be provided by the available PU channels using moment method. Specifically, a closed-from approximation for the distribution of the total amount of data available for SUs over all the available primary channels during any arbitrary interval of time was obtained.

3.2. Primary User Activity Model

In CR networks, SUs shares the radio spectrum with PUs. Higher priority is giving to PUs, and SUs have to vacate the spectrum whenever the PU is detected to avoid any possibility of causing an interference. Hence, the performance of SUs in CR networks is highly dependent upon modeling the behavior of PUs (their traffic characteristics). There are different types of PUs and each type has different traffic model. For example, when traffic is assumed to be bursty (e.g. TV channels) the PU activity pattern in each channel can be modeled as 2-state ON / OFF Markov model where ON-period represents the time when a channel is busy i.e. occupied by PU, and an OFF-period represents the time where a channel is idle (SUs can opportunistically access the channel). ON/OFF periods are assumed to be exponentially distributed with rate parameters λ_{ON} and λ_{OFF} [66–69]. On the other hand, when the traffic of PU is more dynamic and time variant (e.g. cellular networks), the 2-state model might not be the best option. Thus, models as Poisson process [70–73] and First-difference filter clustering model might be more accurate as it consider the short-term fluctuations and the bursty and spiky features of the PU activities [74]. Another widely used model is the $M/G/1$ queue model in which arrivals are Markovian, service times have a general distribution, and the packet arrival process is a Poisson random process with average packet arrival rate λ [8] [75].

3.3. System Model

Our system model in Figure 3 shows a CR base station that multicasts the encoded video sequences to multiple SUs during the idle intervals on subset of the M channels. There are M-PUs with M designated frequency channels; $\mathbf{PU} = PU_1, \ldots, PU_M$, and N-SUs; $\mathbf{SU} = SU_1, \ldots, SU_N$. The primary channel is modeled as a 2-state Markov model. In state 1, the channel is idle and a SU can access the spectrum and transmit with a transmission rate R while in state 0, the channel is busy and occupied by the PU. Figure 4 shows the system model of the m^{th} channel. Primary channels are assumed to be independent.

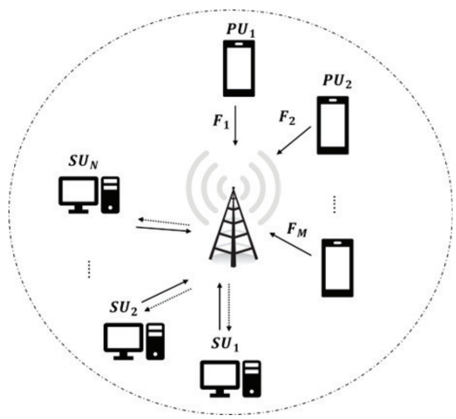

Figure 3: System model.

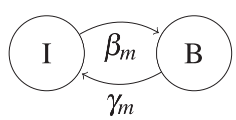

Figure 4: Primary channel model.

3.4. The Distribution of the Total Amount of Data

In this section,the proposed closed-from approximation for the distribution of the total amount of data available for SU over all the available primary channels during any arbitrary interval is presented. The main derivation is adopted from [76], but the equations were adjusted to serve our problem. The accuracy of the obtained closed-form approximation is verified using simulations and numerical investigations.

3.4.1. Statistical analysis. Let $I(t)$ represents the random process of the total amount of data that can be transmitted over all the available channels during an arbitrary interval of time, t. Thus, $I(t)$ can be expressed as

$$I(t) = \int_0^t R(\tau)\, d\tau, \tag{1}$$

and

$$R(t) = \sum_{m=1}^{M} R \times A_m(t), \tag{2}$$

where $R(t)$ is the random process that represents the total rate available over all idle primary channels at time instant t, R is the transmission rate, and $A_m(t)$ is the 2-state Markov process that models the availability of the primary channel with γ and β denoting the transition rates from state 0 to state 1 and from state 1 to state 0, respectively. Now, let's define

$$Z_m(t) = \int_0^t A_m(\tau) d\tau, \tag{3}$$

where $Z_m(t)$ represents the amount of time available at the $m-th$ channel during an arbitrary interval of duration t. Figure 5 illustrates the time space of the system. The amount of time available in each frequency channel $F_1, F_2, \ldots, F_M$ is a random process, then the total amount of time available over all the available primary channels is another random process that is the summation of the individual random processes.

Hence, the total amount of time available over all available channels can be written as

$$Z(t) = \sum_{m=1}^{M} Z_m(t). \tag{4}$$

Therefore, $I(t)$ can be written as

$$I(t) = RZ(t). \tag{5}$$

Once the distribution of $Z(t)$ is obtained, the distribution of $I(t)$ can be easily obtained through transformation of random variables as

$$F_{I(t)}(i) = F_{Z(t)}\left(\frac{i}{R}\right), \tag{6}$$

$$f_{I(t)}(i) = \frac{1}{R} f_{Z(t)}\left(\frac{i}{R}\right), \tag{7}$$

where $F_{I(t)}(i)$ and $F_{I(t)}(i)$ are their cumulative distribution functions (CDFs) of the process $I(t)$ and $Z(t)$. While, $f_{I(t)}(i)$ and $f_{Z(t)}\left(\frac{i}{R}\right)$ are the probability density functions (PDFs).

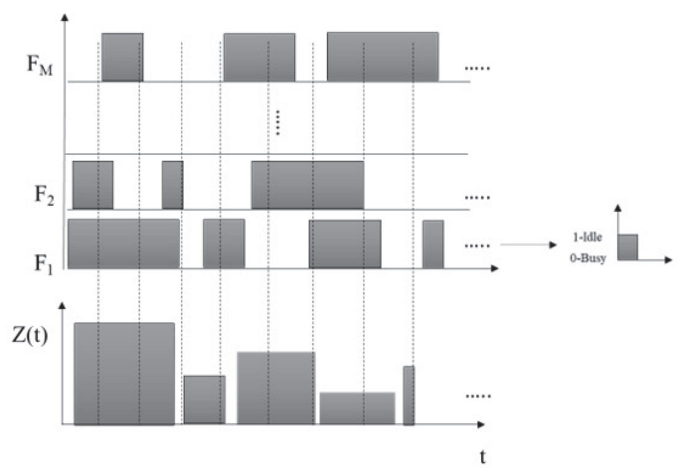

Figure 5: Accumulated time available over M channels.

Due to the difficulty of obtaining the exact distribution of $Z(t)$, the moment matching method can be used to get an approximated version of the distribution. As matching the moments is equivalent to matching the cumulants, we will approximate the distribution through matching its cumulants. To obtain the $n-th$ cumulants we use $\kappa^n = K^n(0)$ Where $K(v)$ is the $n-th$ derivative of the cumulant generating function

(CGF), which is found for $Z(t)$ by $K(v) = ln\left(E\left[e^{vZ(t)}\right]\right)$, where $E(.)$ is the expectation operator.

As the sampled process $A_m(t_j) \sim$ Bernoulli $\left(\frac{\gamma_m}{\gamma_m+\beta_m}\right)$ the process $Z(t)$ can be treated as the limit of a stochastic sequence of a partial sum of Bernoulli RVs. Therefore, $Z(t)$ can be written as

$$Z(t) = \sum_{m=1}^{M} Z_m(t) = \lim_{k\to\infty} \sum_{m=1}^{M} \sum_{j=1}^{k} A_m(t_j)\,\Delta t. \tag{8}$$

When the Bernoulli RVs are independent or uncorrelated the sequence of the partial sum converges to a deterministic function according to the strong law of large numbers. However, in our case the RVs are assumed to be correlated over a short window of time and the sequence of partial sums converges to a distribution that might be a skew normal. From the third cumulant, when $\gamma \neq \beta$, or the time interval t is relatively small compared to $\frac{1}{\gamma} + \frac{1}{\beta}$, the PDF that results from sampling $Z(t)$ can be approximated by a mixture of a skew normal distribution, however, as the number of the accumulated independent channels increases the normal distribution can be used to provide an accurate approximation for the distribution of $Z(t)$ by the central limit theorem. While, when γ and β are reasonably large or approximately when they are equal the normal distribution can be used irrespective of the number of accumulated channels. Based on this and using the Markov property, the PDF of $Z(t)$ can be approximated by

$$f_{Z(t)}(z) = \frac{2}{\omega(t)}\phi\left(\frac{z-\xi(t)}{\omega(t)}\right)\Phi\left(\alpha(t)\left(\frac{z-\xi(t)}{\omega(t)}\right)\right), \tag{9}$$

where ϕ and Φ are the PDF and the CDF of $N\ (0,1)$ distribution, respectively. The parameters of the skew normal part of $Z(t)$ are given by:

$$\omega(t) = \sqrt{\pi\kappa_2(t)\,/\,(\pi - 2\zeta^2(t))},$$

$$\alpha(t) = \zeta(t)\,/\sqrt{1-\zeta^2(t)},$$

and

$$\xi(t) = \kappa_1(t) - \omega(t)\,\zeta(t)\,\sqrt{2/\pi}, \tag{10}$$

where $\zeta^2(t) = \frac{\pi}{2} \times |\kappa_3(t)|^{\frac{2}{3}} / \left(|\kappa_3(t)|^{\frac{2}{3}} + \left(2 - \frac{\pi}{2}\right)^{\frac{2}{3}} \kappa_2(t) \right)$ and $\kappa_1(t)$, $\kappa_2(t)$, and $\kappa_3(t)$ are the first three cumulants of the skew normal part of the distribution of $Z(t)$, where $\kappa_1(t) = E[Z(t)]$, $\kappa_2(t) = E[Z^2(t)] - E^2[Z(t)]$, and $\kappa_3(t) = E[Z^3(t)] - 3E[Z^2(t)]E[Z(t)] + 2E^3[Z(t)]$. Therefore, we need to calculate the first three moments of $Z(t)$ in order to calculate the required cumulants. The first moment is

$$E[Z(t)] = \sum_{m=1}^{M} \int_0^t E[A_m(\tau)]d\tau = \sum_{m=1}^{M} \frac{\gamma_m}{\gamma_m + \beta_m} t, \tag{11}$$

The second moment of $Z(t)$ is obtained as follows

$$E[Z^2(t)] = \sum_{m=1}^{M} \int_0^t \int_0^t E[A_m(\tau)A_m(s)]d\tau\, ds, \tag{12}$$

Clearly, the second moment of $Z(t)$ is simply the correlation of the process $A(t)$. In fact, all higher order moments will depend on how the samples of the process $A_m(t)$ are correlated. Hence, the second moment is

$$E[Z^2(t)] = \sum_{m=1}^{M} \left(\frac{\gamma_m}{\gamma_m + \beta_m} \right)^2 t^2 + \frac{2\gamma_m\beta_m}{(\gamma_m + \beta_m)^4} \times \left(e^{-(\gamma_m + \beta_m)t} + (\gamma_m + \beta_m)t - 1 \right), \tag{13}$$

Similarly, the third moment is obtained by

$$E[Z^3(t)] = \sum_{m=1}^{M} \int_0^t \int_0^t \int_0^t E[A_m(\tau)A_m(s)]d\tau\, ds\, dr, \tag{14}$$

Due to symmetry, the above integration can be simplified by considering the cases where $\tau \leq s \leq r$ then multiplying the result by 3! which is the number of permutation. Thus, the result is

$$E[Z^3(t)] = \sum_{m=1}^{M} \left(\frac{\gamma_m}{\gamma_m+\beta_m}\right)^3 t^3 + \frac{6{\gamma_m}^2\beta_m}{(\gamma_m+\beta_m)^4} t^2 + \frac{6\gamma_m\beta_m^2\left(e^{-(\gamma_m+\beta_m)t}+1\right) - 12{\gamma_m}^2\beta_m}{(\gamma_m+\beta_m)^5} t + \frac{12\gamma_m\beta_m(\gamma_m-\beta_m)\left(1-e^{-(\gamma_m+\beta_m)t}\right)}{(\gamma_m+\beta_m)^6}. \tag{15}$$

Now, using (9), the CDF can be straightforwardly obtained as,

$$F_{Z(t)}(z) = \Phi\left(\frac{z-\xi(t)}{\omega(t)}\right) - 2T\left(\frac{z-\xi(t)}{\omega(t)}, \alpha(t)\right) \tag{16}$$

where $T(.,.)$ is the Owen's T function, and Φ is the CDF of $N(0,1)$ distribution . The distribution of the total amount of data $I(t)$ can be obtained easily by using (6) and (16).

3.4.2. Analytical and simulation results. In this work, Monte-Carlo simulations was used to investigate the accuracy of the proposed distribution in modeling the total amount of data that can be obtained from all the available primary channels. In simulation, wireless channels were assumed to be independent and identically distributed random processes, and a 2-state Markov chain was used to model each channel. In all the presented graphs lines and markers (circles) indicate analytical and simulation results, respectively.

Figure 6 illustrates how the proposed skew normal distribution perfectly matches the PDF of the total amount of time available for all SU, $Z(t)$ for different number of channels M and different sampling time t. Clearly, γ and β highly influence the direction of the skewness of the distribution as it can be noticed from Figures 6(a)-(c). When $\gamma < \beta$ the distribution is skewed left while it is skewed right when $\gamma > \beta$. However, as the number of channels increases the distribution will become more symmetric. In addition, when $\gamma = \beta$ the distribution of $Z(t)$ will always be symmetric irrespective of the accumulated number of channels.

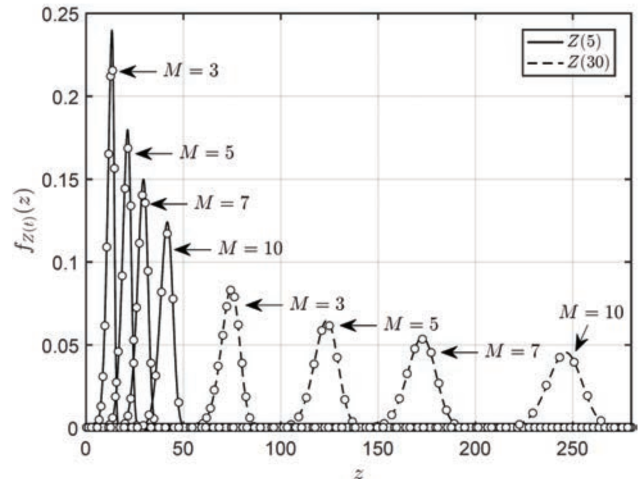

(a) $\gamma < \beta$.

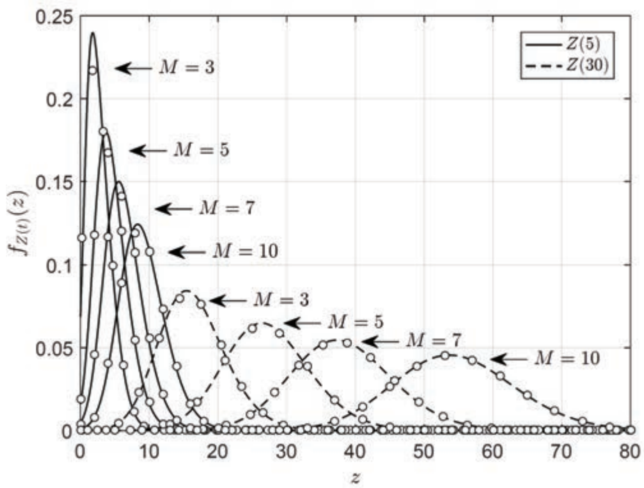

(b) $\gamma > \beta$.

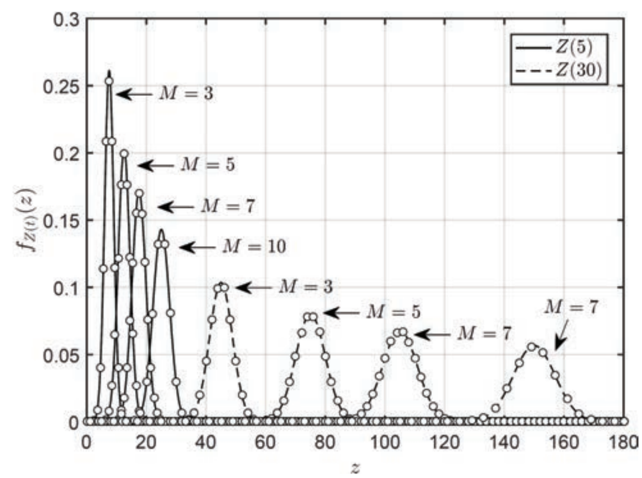

(c) $\gamma = \beta$.

Figure 6: Analytical and simulated PDF of $Z(t)$ for different number of primary channels, different sampled time, and different transition rates.

Chapter 4: LTE-based Cognitive Radio Network

In this chapter, we formulate the problem of streaming scalable video sequences from a base station (BS) to multiple secondary users (SUs) over an LTE-based CR network. The proposed system model and assumptions are introduced first, then rate calculations and resource allocation and streaming algorithms are discussed.

4.1. Problem Formulation

The problem we investigate in this chapter is to implement an LTE-based CR network, solve the problem of resource allocation, and stream SVC video sequences over the proposed system.

4.2. System Model

In our work, we implemented a CR system using an LTE platform, where PUs and SUs share a set of M orthogonal channels with K resource blocks (RBs). An interweave mode of transmission was assumed, where the primary and secondary users can't simultaneously access the CR spectrum. Therefore, once a channel is declared as idle by the BS, it will remain available until the end of a certain period of time denoted as T_{slot} with no interference to the PUs. RBs are scheduled every T_{slot} which is equal to 1 *ms* duration. Equal power allocation is adopted such that all RBs have the same transmission power, which is equal to the maximum power assigned to the base station divided by the total number of RBs [77–79].

The available RBs are allocated to SUs based on their feedback information, which include their buffer occupancies as well as the measured SNR. The channel gain between BS and SU ($h_{Bs,SU}$) is assumed to be constant within each T_{slot}. Micro urban channel model introduced in [80] is adopted in simulation. A distance-based path loss, shadow fading and Rayleigh fading is assumed. Shadow fading is modeled by log-normal random variable and the path loss for the BS-SU link is defined as 36.7 log_{10} $(d[m]) + 22.7 + 26\ log_{10}(f[GHz])$. We assume that the availability of each time slot follows a discrete-time two-state Markov model with a transition probability matrix P_m where m is the channel index. The duration of an idle time slot T_{slot} is assumed to be fixed and equal to TTI.

Once the channel is declared to be idle at any TTI, the BS then schedules the video frames from different coded layers under the constraints of maximum bit budget that is offered to the user and the delay deadline using streaming algorithm. We assess the performance of the proposed video streaming scheme using the Peak Signal to Noise Ratio (PSNR) and average PSNR , which are typically used to quantify the spatial aspect of the video quality. The scalability coding techniques allow the BS to adapt to the dynamic network conditions and the intermittent availability of the PUs' channels to deliver the video sequences with the highest possible quality and minimum discontinuities. Video frames form different coded layers are sent on the available time slots by the BS according to proposed channel allocation and streaming algorithms that will be discussed later. Figure 7 shows the proposed video streaming scenario. In this work, available channels and available RBs will be used interchangeably.

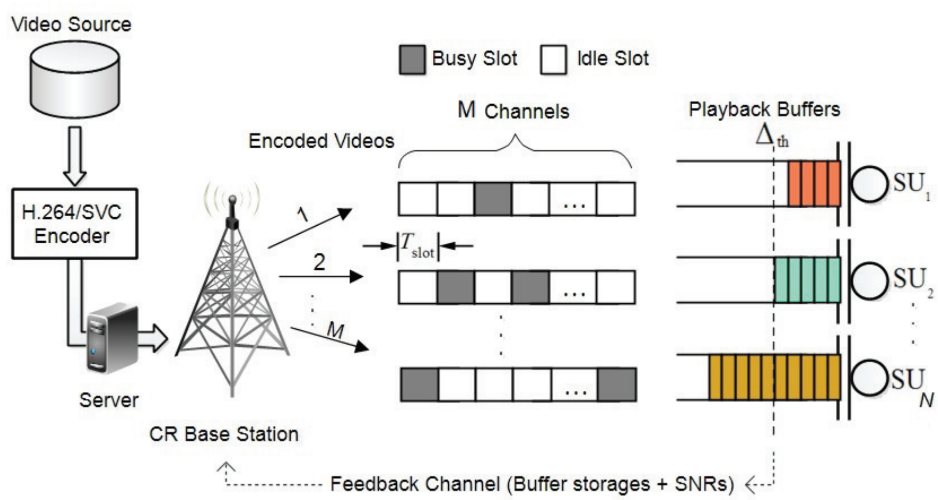

Figure 7: Proposed video streaming scenario.

4.3. Rate Calculation

Considering channel conditions and the minimum required rate by each user, RBs are allocated to each SU in a round robin fashion. Prior to allocation, the feedback channel state information (CSI) are provided to the BS by SUs including their buffer occupancies as well as the measured SNR over each RBs. After that, the BS estimates the number of RBs required by each user using the following metric

$$RB_n^{Req} = \frac{\overline{r_n}}{\frac{1}{N}\sum_{j=1}^{N}\overline{r_j}} \times \frac{R_n^{req}}{\frac{1}{N}\sum_{j=1}^{N}R_j^{req}}, \tag{17}$$

where $\overline{r_n}$ is defined as

$$\overline{r_n} = \frac{1}{K}\sum_{k=1}^{K} SNR_{n,k} \tag{18}$$

$SNR_{n,k}$ is the signal to noise ratio of user n on RB k over a specific T_{slot}, K is the total number of available RBs, and R_n^{req} is the required throughput of user n.

The achievable rate of any user will depend on the nature of its communications link and it can be calculated as

$$R_n^{achievable} = B_n log_2(1 + \frac{P_{BS}|h_{BS,SU}|^2}{N_0 B_n}) \tag{19}$$

where N_0 is the Additive White Gaussian Noise (AWGN) power spectral density and B_n is the bandwidth allocated to SU_n and it can be found using

$$B_n = K_n \times BW \tag{20}$$

where K_n is the number of resource blocks allocated to user n and BW represents the RB bandwidth in LTE, which is 180 kHz.

In LTE network, rate calculations may follow two approaches, one based on Shannon's capacity theorem, and the second scheme based on LTE Transport Block (TB) structure.

1. Shannon's capacity can be used to predict the maximum theoretical rate of information transmitted through a channel using:

$$R_n^{Theoretical} = B_n log_2(1 + SNR_n) \tag{21}$$

2. Based on LTE standard specifications, the rate can be calculated as follows:

   - 1 Time-slot (1 RB) occupies 0.5 ms.

- There are 7 modulation symbols per 1 time-slot.
- 1 Modulation symbol is used to transfer x bits, based on modulation scheme (QPSK, 16-QAM, or 64-QAM).

Therefore, based on LTE standard Release 13 each user is assigned a Transport Block (TB) over the system physical layer to transmit data. Each TB is transmitted over 1 TTI (T_{slot}). The size of a TB, known as Transport Block Size (TBS), is calculated based on the Modulation and Coding Scheme (MCS) and the number of RBs allocated to a SU by the BS as defined in the LTE Technical Specification in [62] Section 7.1.7.1,(Table 3). To find the rate, the BS collects the CQI from the feedback sent (measured SNR) by the SU, then the BS maps the measured SNR to CQI [81], (Table 2). All RBs allocated to the same user should be assigned the same MCS index I_{MCS}. The size of TB to be allocated to a SU is found based on a mapping relation between I_{MCS}, TBS index (I_{TBS}) and the number of resources $RB_{n,t}^{Req}$ allocated by BS as defined in the LTE Technical Specification. Consequently, the rate is found by

$$R_{n,t} = f(I_{MCS_{n,t}}, RB_{n,t}^{Req}) \tag{22}$$

where $f(I_{MCS_{n,t}}, RB_{n,t}^{Req})$ is a mapping function between the number of resource blocks allocated and TBS.

4.4. Dynamic Resource Allocation

The goal of our proposed video streaming algorithms is to maintain continuity of the playback at the SUs end and enhance the quality of the streamed scalable video sequences. Two algorithms are introduced to achieve the goal; channel allocation and streaming algorithms. The channel allocation algorithm is designed to adaptively sense and allocate the available channels (RBs). While, streaming algorithm is responsible for scheduling video frames within the slots of the allocated RBs based on certain constrains (frames deadlines).

4.4.1. Allocation algorithm. The available RBs identified by the BS are allocated to SUs based on their feedback information, received regularly every T_{slot} (TTI) on a reliable error free reverse channel, which includes their buffer occupancies as well as the measured SNR of different RBs. Three allocation schemes are applied; buffer-based, SNR-based, and joint buffer and SNR based where the buffer state and the reported SNR are used to establish the allocation policy. The pseudocodes for the allocation techniques used are explained in Algorithms (1),(2), and (3).

4.4.1.1. Buffer-based allocation. The BS allocates the available RBs to SUs by comparing their buffer occupancies with a predefined occupancy threshold Δ_{th} to determine the urgency of sending the video frames to each SU. Thus, SUs with lower occupancies are served first to avoid starvation, however, they may not be allocated a good quality RBs. The algorithm follow the two following scenarios:

- All SUs have their buffer occupancies larger than the threshold ($\Delta_n > \Delta_{th}$, $\forall n$ = 1,2, .., N), or all their buffer occupancies are below or equal the threshold $\Delta_n \leq \Delta_{th}$, $\forall n$ = 1,2, .., N. In this case the available RBs are equally allocated over all the SUs in a Round Robin fashion, starting with the SU with the minimum occupancy. The procedure is repeated until all the available RBs are fully allocated to the SUs.
- Some SUs are underflowing ($\Delta_n \leq \Delta_{th}$ n = 1, 2, .., N_u) where $N_U \leq N$, thus, the available RBs are only allocated to the needed SUs starting with the SU of the minimum occupancy. The procedure is repeated until all the available RBs are fully allocated to the SUs.

4.4.1.2. SNR-based allocation. The second scheme is solely based on the reported SNR of the different RBs as seen by the SUs. Each SU reports to the BS a vector of the measured SNR over all the available RBs, $SNR_n = [SNR_{n,1}, SNR_{n,2}, ..., SNR_{n,K}]$. To elaborate, assume that the n^{th} SU has the largest SNR reported for the k^{th} RB, thus, $SNR_{k,n}$ = max $(SNR_{k,1}, SNR_{k,2}, .., SNR_{k,N})$. Hence, the BS will allocate the k^{th} RB to the n^{th} user who can achieve the maximum quality when assigned the RB. If two or more SUs have the same level of quality on a RB, then that RB is randomly allocated to one of them. While the allocation that is based only on reported SNRs may assign the RBs with good quality to SUs, the ignorance of the buffer state may result in starvation and interruptions in the playback for some SUs. The procedure is repeated until all the available RBs are fully allocated to the SUs.

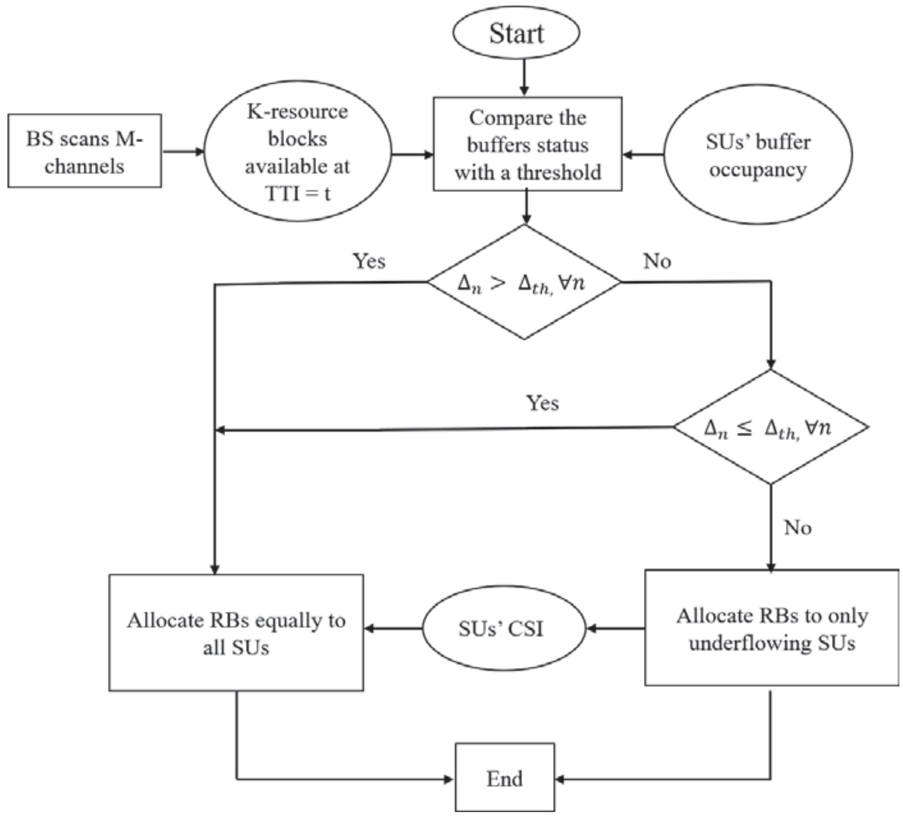

Figure 8: Joint based channel allocation algorithm flow chart.

4.4.1.3. Joint allocation. The third scheme is a joint scheme where allocation is based on both channel quality and buffer occupancy. The BS allocates SUs with buffer occupancies below the threshold (Δ_n) the RBs with the maximum quality. Figure 8 summarizes the algorithm.

4.4.2. Streaming algorithm. Our video sequences are encoded using the H.264/SVC encoding standard into one BL and two ELs. Receiving only BL provides the basic accepted quality level, however, the quality level can be enhanced by transmitting more ELs. If the buffer occupancy of a SU is below the threshold , a base layer is transmitted to maintain the continuity. After all BLs for all the scheduled SUs are transmitted, if there still available RBs ELs will be scheduled. EL layers will be transmitted when all lower dependent layers have been transmitted and correctly received. To decide how many EL layers to transmit, the number of layers L of a frame f should be received before their deadlines. This is done by adding the current time slot t to the time required

Algorithm 1: Buffer-Based Allocation

Input : K, $\Delta_n, n = 1, 2, ..., N.$, RB_n^{Req}
Output: $RB_{SU_1}, RB_{SU_2}, ..., RB_{SU_N}$ // Vector of RBs allocated to each SU.
Set : $\Delta_{th} = x$; // Buffer threshold.

```
if Δ_n > Δ_th or Δ_n ≤ Δ_th, ∀n = 1,2, .., N then
    sort (Δ_1, Δ_2, ..., Δ_N) // sort in the ascending order. Allocate required RBs
      to all SUs on Round Robin basis;
    K ← K - RB_n^Req // the remaining available RBs
end if
else if Δ_n ≤ Δ_th, n = 1, 2, .., N_u then
    sort (Δ_1, Δ_2, ..., Δ_{N_u}) // sort in the ascending order. Allocate required
      RBs to all SUs on Round Robin basis;
    K ← K - RB_n^Req// the remaining available RBs
end if
```

Algorithm 2: SNR-Based Allocation

Input : K, $SNR_n, n = 1, 2, ..., N$, RB_n^{Req}.
Output: $RB_{SU_1}, RB_{SU_2}, ..., RB_{SU_N}$ // Vector of RBs allocated to each SU.

```
for k = 1, 2, .., K // for each available RB do
    SNR_{k,n} = max(SNR_{k,1}, SNR_{k,2}, .., SNR_{k,N}); // Allocate the required RBs
      to SU_n with max SNR
    K ← K - RB_n^Req // the remaining available RBs
    SNR_(:,n) = 0 // remove SU_n
end for
```

to transmit ELs as below:

$$t + \frac{(\sum_{l=1}^{L} b_n^{f,l})}{\overline{r_n}} < display\ time\ of\ frame\ f \tag{23}$$

where $b_n^{f,l}$ is the number of bits in the l^{th} EL that is corresponding to frame f an $\overline{r_n}$ is the average rate of the n^{th} SU.

4.5. Simulation Results

In this chapter, we evaluate the performance of the proposed architecture through extensive simulations. We consider a single LTE cell with a BS located at the center of the cell with a radius of 500 m and has 3 PUs. PUs and SUs are distributed randomly.

Algorithm 3: Joint buffer and SNR Based Allocation

Input : K, $SNR_n, n = 1, 2, ..., N$, RB_n^{Req}.
Output: $RB_{SU_1}, RB_{SU_2}, ..., RB_{SU_N}$ // Vector of RBs allocated to each SU.
Set : $\Delta_{th} = x$; // Buffer threshold.

if $\Delta_n > \Delta_{th}$ *or* $\Delta_n \leq \Delta_{th}$, $\forall n$ = *1,2, .., N* **then**
  sort $(\Delta_1, \Delta_2, ..., \Delta_N)$ // sort in the ascending order. Allocate the required RBs to all SUs on Round Robin basis;
  for $k = 1, 2, .., K$ // for each available RB. **do**
    $SNR_{k,n}$ = max$(SNR_{k,1}, SNR_{k,2}, .., SNR_{k,N})$; Allocate the required RBs to SU_n with max SNR;
    $K \leftarrow K$ - RB_n^{Req} // the remaining available RBs
    $SNR_{(:,n)}$ = 0 // remove SU_n
  end for
end if
else if $\Delta_n \leq \Delta_{th}$, *n = 1, 2, .., N_u* **then**
  sort $(\Delta_1, \Delta_2, ..., \Delta_{N_u})$ // sort in the ascending order. Allocate RB to only in need SUs on Round Robin basis according to their ascending order;
  for $k = 1, 2, .., K$ // for each available RB. **do**
    $SNR_{k,n}$ = max$(SNR_{k,1}, SNR_{k,2}, .., SNR_{k,N_u})$; Allocate required RBs to SU_n with max SNR;
    $K \leftarrow K$ - RB_n^{Req}// the remaining available RBs
    $SNR_{(:,n)}$ = 0 // remove SU_n
  end for
end if

Available RBs are uniformly distributed among PU channels by the BS. For example, if the BS operate at 20 MHz, thus, in total there are 100 RBs available to be distrusted among the 3 PUs. The total amount RBs available for SUs depends on the total available PUs' channels. If only one PU channel available then 33 RBs are available, if 2 PUs' channels are available then 66 RBs are available, and if the three PUs' channels are available then 100 RBs.

4.5.1. Simulation parameters. In this section, MATLAB has been used as a simulation environment and the numerical results are averaged over 50 runs, each run last for 30 seconds. In all our simulations, the BS transmits video sequences that are encoded to N = $\{3, 8, 15\}$ SUs over M = 3 PU' channels that are opportunistically accessed by SUs according to the discrete-time two-state Markov chain model with transition matrix P = [0.957 0.043 ;0.9 0.1] with limiting probability π_1 of 30%. The transmission power of the BS to the maximum value 46 dBm (39.8 W). Moving to video streaming parameters, two video sequences have been used from trace file library; Sony Demo and Ghandhi. Video sequences are encoded into one BL and two ELs with playback rate of 30 frames per second, and the GoP structure of the layer is G16B15.

4.5.2. Streaming single-layered video. We used the H.264 single layer encoded trace file for the video sequences Sony Demo with playback rate of f_p = 30 frame per second. The GoP structure of the layer is G16B15. Our main objective is to maintain continuous playback at the SUs end by avoiding starvation moments at the buffer, to provide SUs with the best possible channel quality, and maximum guaranteeing fairness among SUs. To evaluate the performance of proposed allocation schemes, two metrics were applied: Jain's fairness index and the average buffer occupancy per user in frames. Jain's fairness index is a metric that is used in network engineering to determine fairness among users. The result ranges from $\frac{1}{N}$ (worst case) to 1 (best case). Jain's fairness index is calculated by:

$$J(R_{SU_1}^{Req}, R_{SU_2}^{Req}, \ldots, R_{SU_N}^{Req}) = \frac{(\sum_{i=1}^{N} R_{SU_i}^{Req})^2}{N \times \sum_{i=1}^{N} (R_{SU_i}^{Req})^2} \tag{24}$$

In Figure 9 fairness is calculated using Eq. 24. Two scenarios were applied for the case of using the reported SNR as an allocation scheme, greedy SNR and SNR-based allocation. The only difference between the two techniques is that in greedy SNR, SUs can be allocated RBs as long as they report the highest SNR during TTI. However, in the other technique, SUs could be assigned RBs only once in every TTI. Greedy SNR is the worst for all the cases, thus it will be ignored. Whereas, the joint buffer and SNR based technique outperforms when the number of SUs decreases as in Figures 9 (a), 9 (b) and 9 (c). Buffer-based allocation technique seems to have comparable performance to the joint buffer and SNR based when the number of SUs is equal to 15 and 8 as in Figures 9 (a) and 9 (b) .

Figures 10 (a), 10 (b) and 10 (c) show the effect of the limiting (i.e. steady state) probability of finding channel m as idle (i.e. $\pi_{1,m}$) on the average buffer occupancy per user. In this test, the number of RBs was fixed to be 6 and the simulation was run for different number of SUs $\{3, 8, 15\}$. We notice that joint buffer and SNR based approach outperforms the SNR and buffer-based in most of the cases. Also, increasing the number of SUs decreases the average number of frames at SUs' buffer. Such behaviour is expected as the number of shared resources is fixed. Also, we notice that increasing $\pi_{1,m}$ will increase the average number of frames at SUs' buffer which is expected as the probability of the channel being available increase and more transmission can occur .

Figures 11 (a), 11 (b) and 11 (c) show the effect of increasing the number of RBs on the average number of frames at SUs' buffer. Based on Figure 11, we again notice that SNR-based scheme performs the worst. The reason is that our main objective which is avoiding buffer underflow is completely ignored when BS allocates RBs among SUs. The allocation is completely done based on the reported SNR irrespective of the buffer state. To understand this more, lets assume the following scenario: there are only two active SUs in the network; SU_1 and SU_2. Lets assume that SU_1 has enough frames at the buffer ($\Delta_1 >> \Delta_{th}$) and SU_2 is starving ($\Delta_2 < \Delta_{th}$), however, SU_1 reports better SNR, thus the BS will allocate the available RBs to SU_1 and not to the starved user SU_1. On the other hand, we can notice that joint buffer and SNR based scheme performance is comparable and sometimes better than the buffer-based scheme in almost all the cases. The reason is that our main objective is met by maintaining a number of frames at buffer as well as taking into consideration the SNR seen by the user to guarantee a successful transmission. Another important observation that when the number of SUs increases from 3 to 15 the performance gap between each scheme increases and this shows that the joint buffer and SNR based is definitely outperforming buffer-based scheme. Also, we can notice that the trend is more obvious when the maximum number of available RBs is small (e.g. 15 and 25) and less obvious for bigger number of available RBs. The reason is when there are plenty of resources available there are less compromises to be done, and all the users get the chance to meet the objective of avoiding starvation in both schemes. On the other hand, when the number of available RBs is restricted the joint buffer and SNR based outperforms. This shows that under limited resources and when more SUs are active, joint buffer and SNR based technique performance is the best.

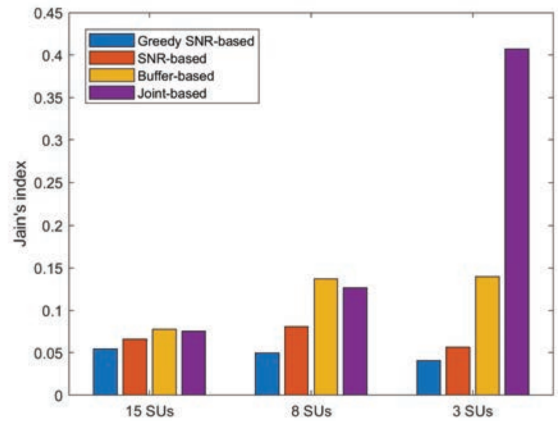

(a) Jain's index when a maximum of 6 RBs available.

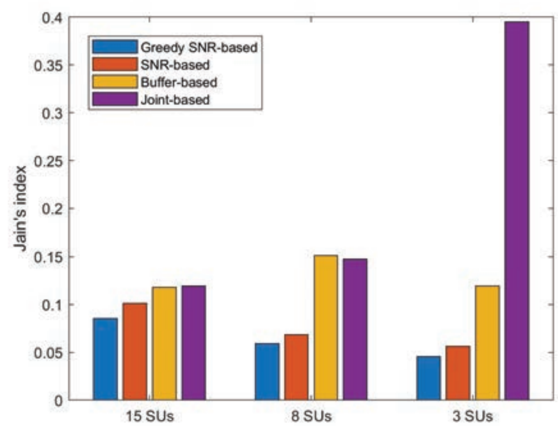

(b) Jain's index when a maximum of 15 RBs available.

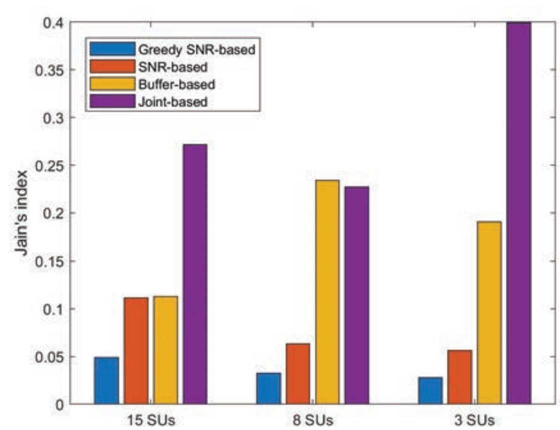

(c) Jain's index when a maximum of 25 RBs available.

Figure 9: Jain's index for greedy SNR, SNR, buffer, and joint buffer and SNR based allocation techniques Vs. the number of active SUs for different number of available RBs.

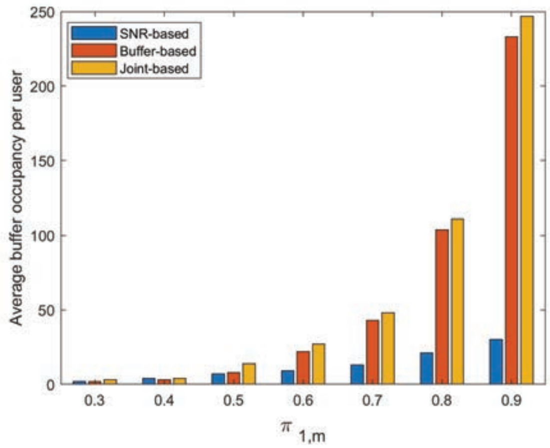

(a) SUs = 3.

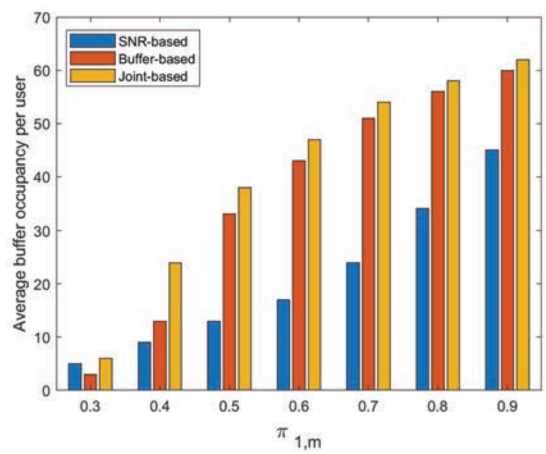

(b) SUs = 8.

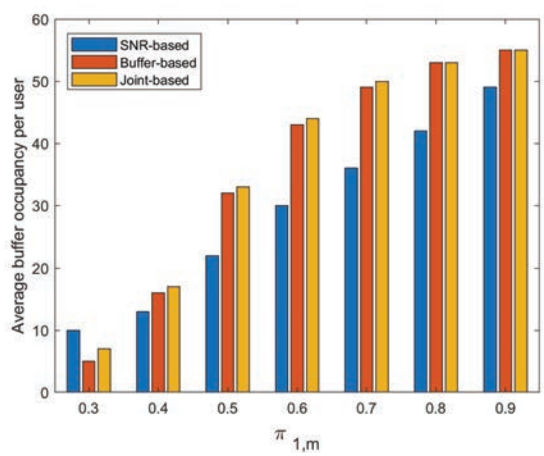

(c) SUs = 15.

Figure 10: The effect of probability of PUs' channels availability on the number of frames at the SUs' buffer.

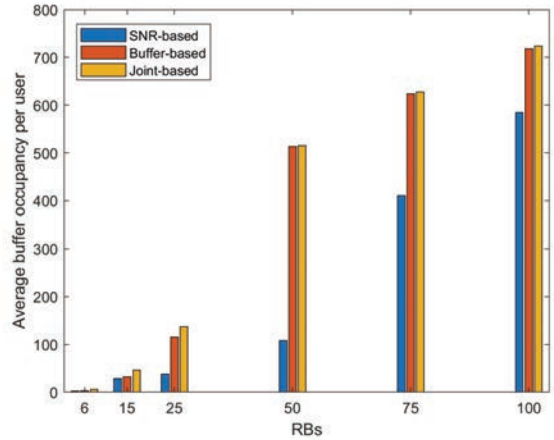

(a) SUs = 3.

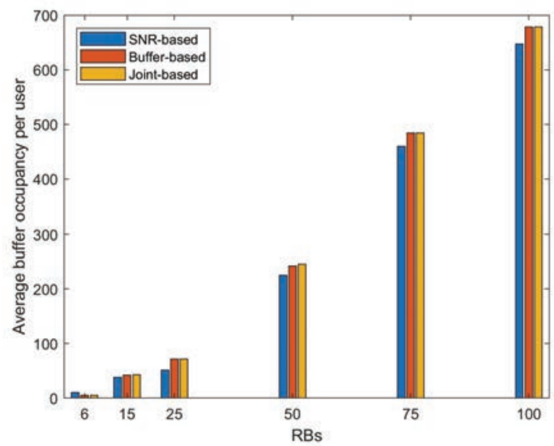

(b) SUs = 8.

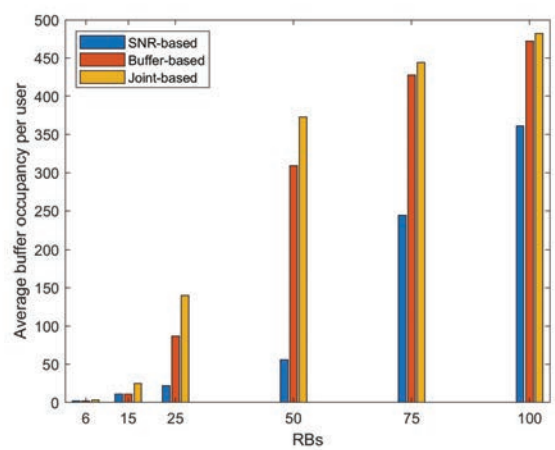

(c) SUs = 15.

Figure 11: The effect of the number of RBs on the average buffer occupancy per user.

4.5.3. Streaming SVC video. In this section, all previous network set up was applied. PUs and SUs are distributed randomly in the network. Available RBs are uniformly distributed among PU channels by the BS and total amount of RBs available for SUs depends on the total available PUs' channels. If one PU channel available, then 33 RBs are available, if 2 PUs' channels then 66 RBs are available, and if the three PUs' channels then 100 RBs. Coarse-Grained video sequences (CGS) are used, Sony Demo and Ghandhi video sequences that consist of 250 total number of frames which is encoded into one BL and two ELs. The resolution of the videos is $352x288$, GoP pattern is $G16B15$, and 30 frame/sec. The evaluation metric used to compare the performance of the three allocation method is PSNR. Previously, we explained the effect of changing the number of available RBs (LTE channel bandwidth) and as expected, increasing the number of RBs increases the opportunity of transmitting video frames. Thus, in this section we only study two case scenarios: operating at 20 MHz (maximum of 100 RBs available) and at 3 MHz (maximum of 15 RBs available). Buffer threshold (Δ_{th}) is set to 5 frames .

Figure 12 shows the average PSNR of the received video when BS operates at 20 MHz, and Sony Demo video sequences are transmitted to all SUs. Comparing Figures 12 (a),12 (b), and 12 (c) we can notice that increasing the number of SUs from 3 to 15 decreases the quality of the received video as less resources will be available for each use. In addition, we can notice that the worst performance in Figures 12 (a),12 (b), and 12 (c) was achieved by SNR-based and this is similar to the conclusion we got in the section 4.5.2. The reason is due to the unfairness of the algorithm where RBs are allocated based on only quality seen by SUs irrespective of their buffer state and the urgency of receiving frames. Thus, SUs who are not in need (not in starvation mode) can continue to receive RBs as long as the maximum quality RBs are seen by them. The Avg. PSNR value in SNR allocation reflects that on average users were able to maintain the minimum quality (as if receiving only the base layer) with PSNR of 37 dB. However, on a user basis some SUs were not even able to be allocated any RBs due to their poor CSI reported as we will show later. Moreover, on average, all SUs were able to receive the video with the highest quality (original quality: receiving both ELs) when joint buffer and SNR based allocation was applied as seen in Figure 12 (a) with an average PSNR of 57 dB. Similar quality was achieved using buffer-based allocation, but there was a slight drop in quality at frame 100, which reflects that some SUs were not able to receive the two ELs due to lack of available RBs at this T_{slot}. Moreover, in Figure 12 (b), when increasing the number of available SUs, joint buffer and SNR based was clearly outperforming buffer-based. There was huge degradation in quality using buffer-based allocation. The reason is due to the ignorance of the RBs' quality. SUs with the lowest buffer occupancy are guaranteed to be served first, however, they are not guaranteed to get a good quality RBs that can support their required rate and this may result in starvation and interruptions in the playback. On the other hand, this is not the case for joint buffer and SNR based as the buffer state and quality of RBs are considered while allocation is performed. Figure 12 (c) shows the achieved Avg. PSNR when the number of SUs is increased to 15 SUs. Although the performance trend of buffer and joint buffer and SNR based is similar, the joint buffer and SNR based performance shows that more SUs were able to receive frames with higher quality, and this reflects that even when the number of RBs to be allocated to each SUs decreased (as number of SUs increased) the joint buffer and SNR based allocation was quantitatively and qualitatively better. The reason of the deep drop in some frames is due to their large sizes (BLs and ELs) and the limited available resources .

Figures 13 shows the average PSNR of the received video when BS operates at 20 MHz, and Ghandhi video sequences are transmitted to all SUs. Comparing the results obtained from Figure 12 and Figure 13, we can notice that the general trend was similar. The joint buffer and SNR based allocation outperform the other two schemes in most of the cases and SNR allocation achieved the minimum performance. However, we can notice that the Avg. PSNR was decreasing when the number of SUs increases in the case of SNR allocation, which was not the case when Sony Demo video sequences were used. The reason that Ghandhi video sequences have larger frame size, that is why even the minimum quality (receiving only BLs) was not achieved by some SUs when the number of SUs is increased .

Figure 14 shows the average PSNR when the BS operates at 3MHz (maximum of 15 RBs available) for Sony Demo video sequences. Obviously, there is a huge degradation in the received video quality compared with Figure 12 which is expected as the number of RBs decreased. Generally, the same trend is happening where SNR-based had the worst performance and the joint buffer and SNR based performed the best. In Figures 14 (b) and (c) we can notice that SUs using SNR allocation are suffering from huge degradation in quality (not even receiving BLs). The first reason is due to the very limited number of RBs (15 RBs if the 3 PUs' channels available) available for SUs, by which the level of competition among SUs is increased. The second reason is due to the unfairness of the algorithm itself as explained earlier. While buffer and joint allocation are having comparable performance. On the other hand, joint buffer and SNR based allocation shows slightly better performance than buffer-based in the three cases. Figure 15 shows the average PSNR when the BS operates at 3MHz (maximum of 15 RBs available) for Ghandhi video sequences. Similar trend to Figure 14 was achieved .

To study this more, we selected a single user to see how each allocation perform for a single case and not on average as seen in Figures 12,14, 13, and 15. We selected the user with the ID number SU_2 when Sony Demo video sequences were transmitted and we monitored the changes that occurred when more SUs joined the network for the three allocation schemes. For Figure 16 (a), SU_2 experienced similar conditions (highest quality and smooth continuity) when buffer and joint buffer and SNR based allocation were used. While, when SNR allocation was used, SU_2 was only able to watch its video sequences in the basic quality (only BLs were received). While, when the number of available SUs increases, the joint buffer and SNR based allocation outperform the buffer-based as seen in Figures 16 (b) and 16 (c). Figures fig:PSNRsu215 (a), (b), and (c) shows the quality received by SU_2 when the BS operates at 3 MHz (with maximum of 15 RBs available). Again, we can notice that joint buffer and SNR based allocation offered better quality to SU_2. Also, Figures 17 (b) and (c) explain the degradation in the average quality seen in Figures 14 (a) and (b), as SU_2 was only able to receive only 20 frames in case of having 8 SUs active and 40 when 15 SUs were active. This shows that some SUs were not able to receive the full video sequences and get in starvation mode. Such case is not applicable in the use of joint and buffer based, and thus, they outperformed SNR in all the scenarios.

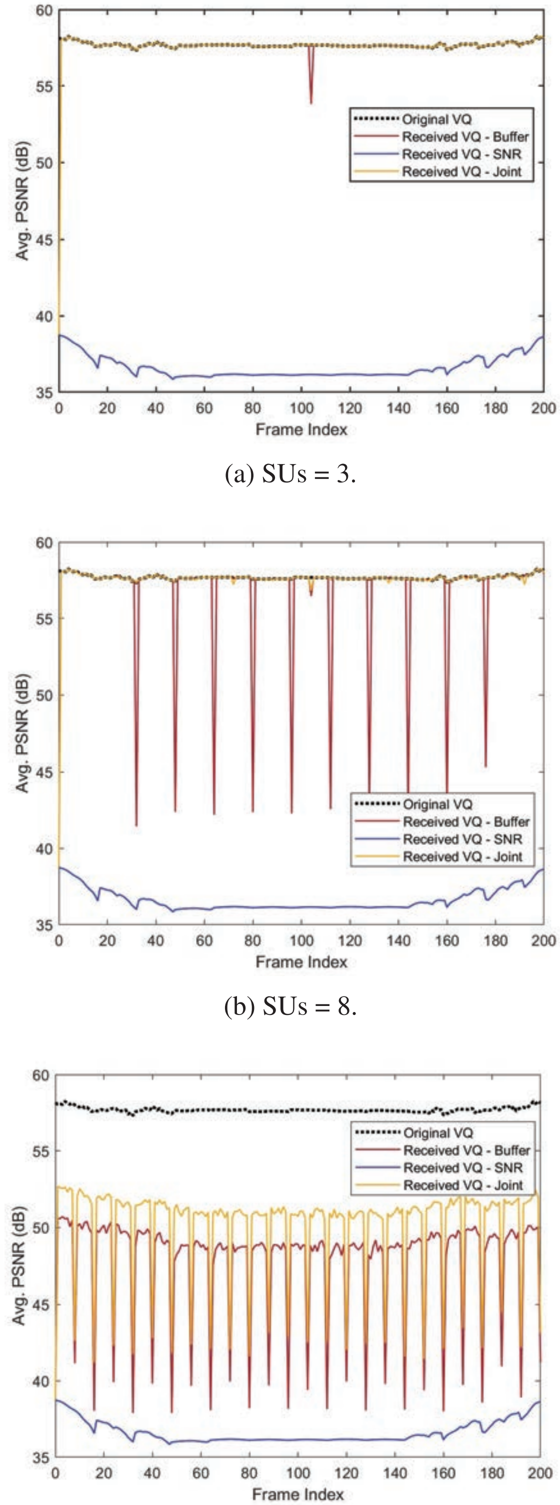

(a) SUs = 3.

(b) SUs = 8.

(c) SUs = 15.

Figure 12: Average PSNR when a maximum of 100 RBs (20 MHz) available (Sony Demo video sequences).

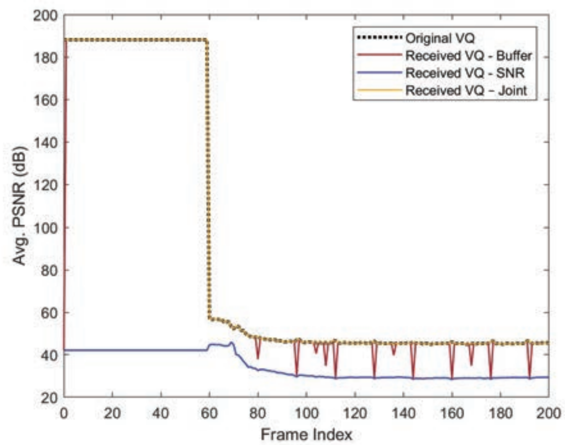

(a) SUs = 3.

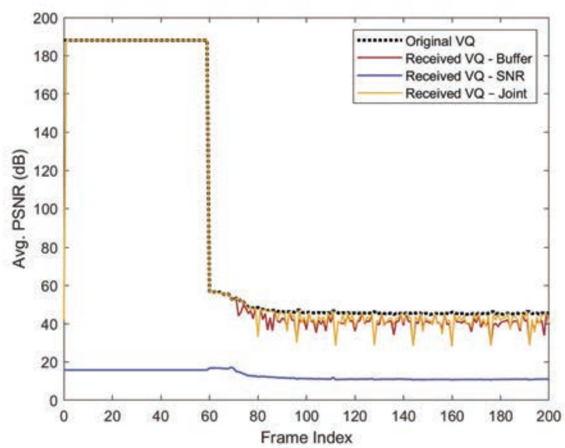

(b) SUs = 8.

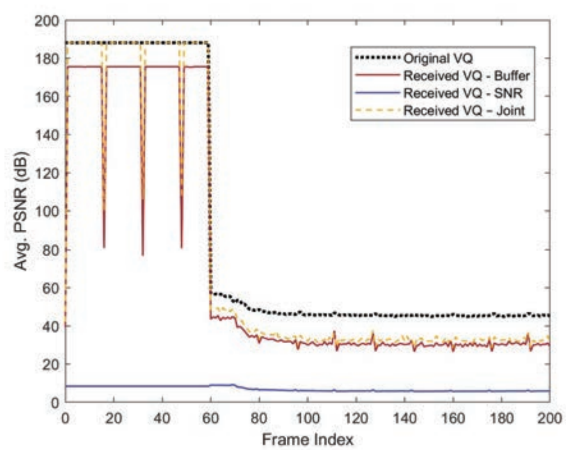

(c) SUs = 15.

Figure 13: Average PSNR when a maximum of 100 RBs (20 MHz) available (Ghandhi video sequences).

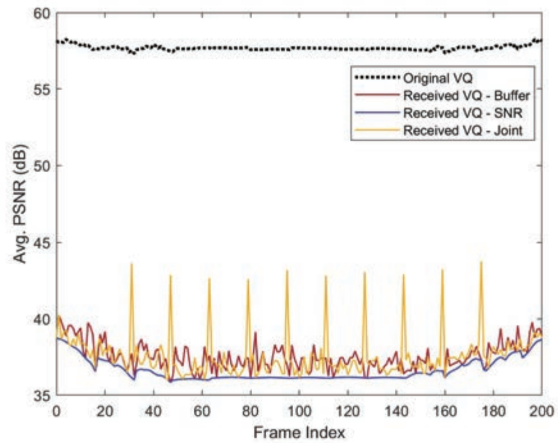

(a) SUs = 3.

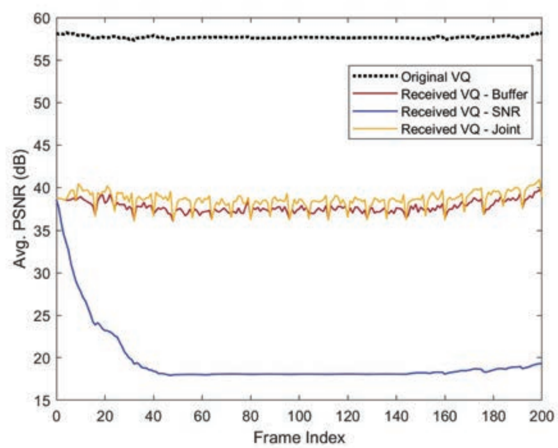

(b) SUs = 8.

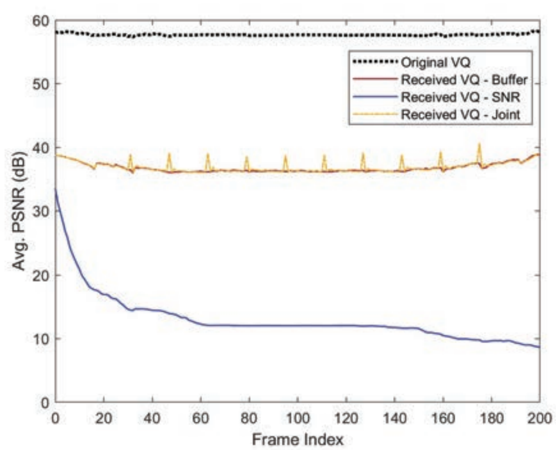

(c) SUs = 15.

Figure 14: Average PSNR when a maximum of 15 RBs (3 MHz) available (Sony Demo video sequences).

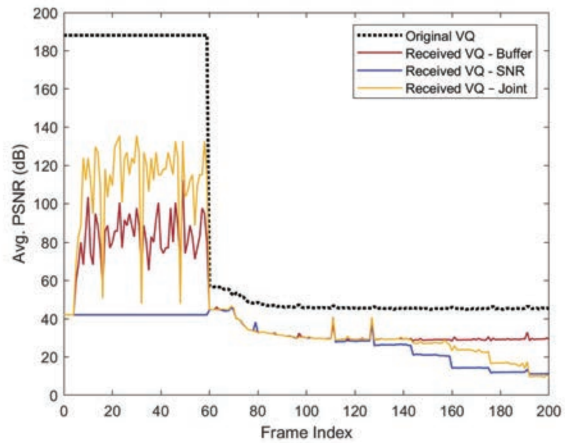

(a) SUs = 3.

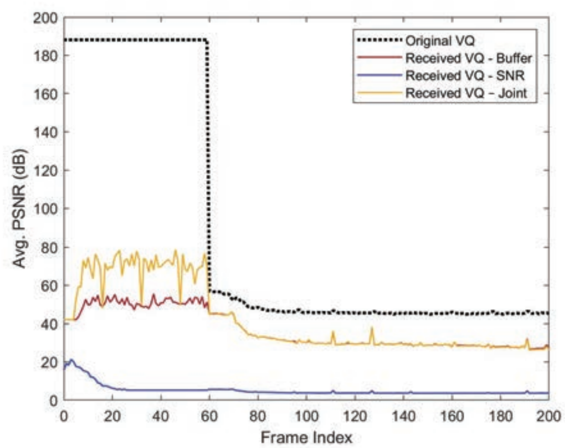

(b) SUs = 8.

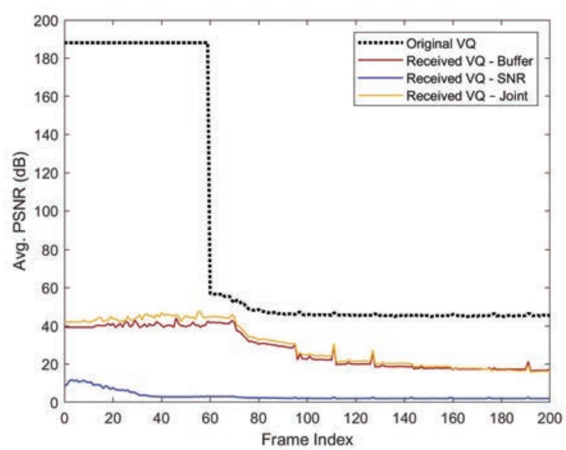

(c) SUs = 15.

Figure 15: Average PSNR when a maximum of 15 RBs (3 MHz) available (Ghandhi video sequence).

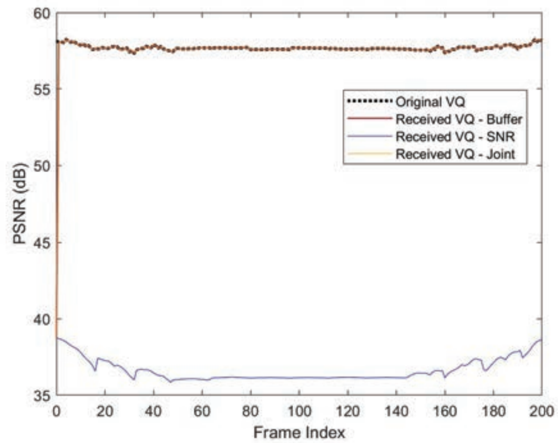

(a) SUs = 3.

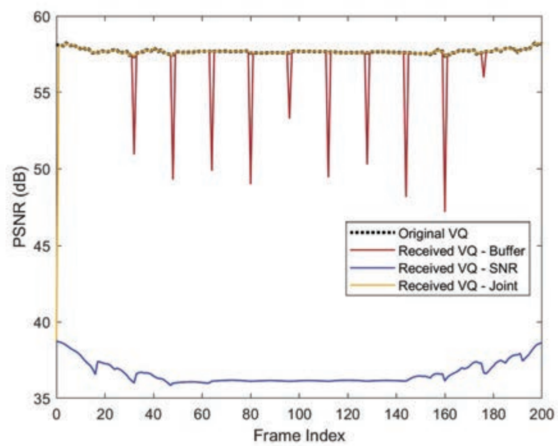

(b) SUs = 8.

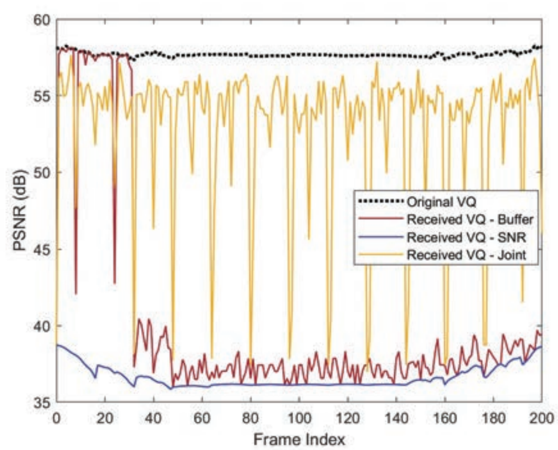

(c) SUs = 15.

Figure 16: The PSNR of SU_2 when a maximum of 100 RBs (20 MHz) available (Sony Demo video sequences).

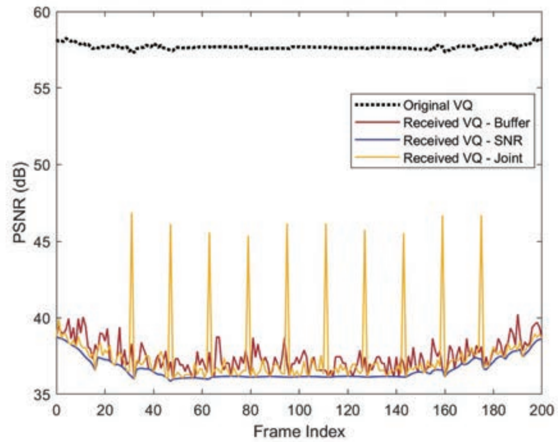

(a) SUs = 3.

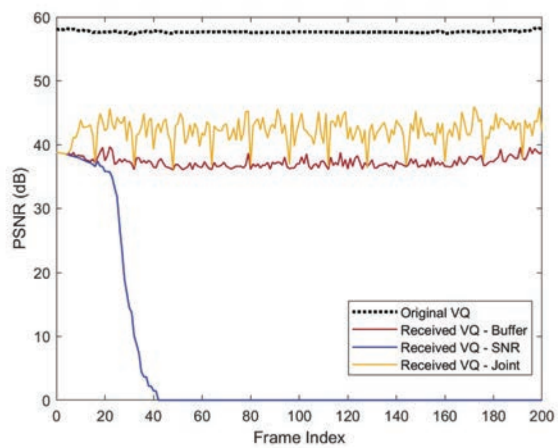

(b) SUs = 8.

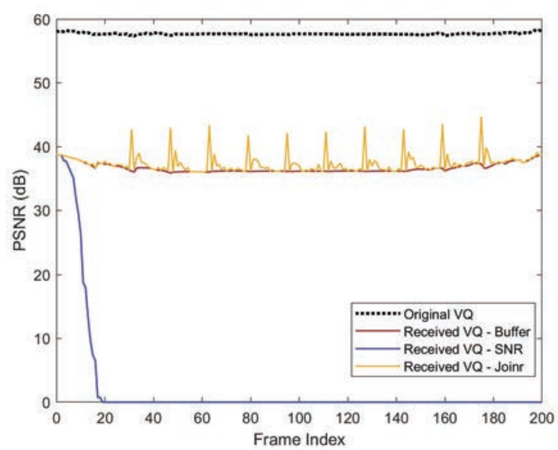

(c) SUs = 15.

Figure 17: The PSNR of SU_2 when a maximum of 15 RBs (3 MHz) available.

Chapter 5: Conclusion and Future Work

5.1. Conclusion

Cognitive Radio Networks (CRNs) were introduced as a promising solution for an efficient spectrum utilization by enabling interactive wireless users to sense and learn the surrounding environment and correspondingly adapt their transmission strategies. In an effort to mitigate spectrum scarcity problem, cognitive radio (CR) technology was proposed as a key solution.

The focus of this thesis is moving toward two parallel directions. Firstly, to quantify the total amount of data that can be provided by the available PU channels using moment method as in Chapter 3. Secondly, to employ an LTE-based CR network as in Chapter 4. In Chapter 3, a closed-from approximation for the distribution of the total amount of data available for SUs over all the available primary channels during any arbitrary interval of time is obtained. In Chapter 4, three resource allocation algorithms are proposed to efficiently allocate the available resources among SUs. The goal is to avoid buffer starvation and maintain continuous playback at the SUs end with the maximum possible quality. SVC video coding is used to provide the video with high quality to SUs with good channel conditions while maintaining the basic video quality for SUs experience bad conditions.

Simulation and analytical results from Chapter 3 proved the accuracy and flexibility of the proposed closed-form approximation of the distribution of $Z(t)$ in quantifying the total amount of data available for transmission. In addition, simulation from Chapter 4 aim to guarantee the continuity of the video playback at the SUs end with acceptable perceptual quality when an LTE-based CR network is employed. To achieve such a goal, a scalable video coding technique is considered to adapt to the dynamic nature of the PUs' channels. Scalable video coding is employed to enhance the quality of the received video by transmitting ELs of the video frames if the conditions set by the streaming algorithm are met. The complexity of the proposed approach is reduced compared to other source rate control approaches as it doesn't require any reconfiguration for the codec parameters. Three allocation schemes (Buffer, SNR, Joint) are proposed and their performance was compared using Jain's index, average buffer occupancy per user, and average PSNR. In summary, we found that joint buffer and SNR based allocation outperformed the other approach for all the different proposed scenarios.

5.2. Future Work

The work in this thesis can be extended in multiple direction. The obtained approximation of the distribution of the total amount of data can be used to devise a rate control mechanism with the objective of maintaining continuous playback at the SUs end while streaming multimedia applications. For the proposed LTE-based CRN, the system model can be extended to a more complicated scenario where there are multiple LTE cells instead of single cell. Another possible extension is by investigating the effect of packet loss on frame quality when the loss is larger than the tolerance level at the decoder.

References

[1] I. F. Akyildiz, B. Lo, Y. Tachwali, A. S. Cacciapuoti, M. Caleffi, W. Y. Lee, and K. R. Chowdhury. (2006, June) Cognitive radio networks. Internet. [Online]. Available: http://bwn.ece.gatech.edu/CR/projectdescription.html [Accessed: Nov. 30, 2018].

[2] C. Cox, *An introduction to LTE: LTE, LTE-advanced, SAE and 4G mobile communications*, 1st ed. Weinheim: John Wiley & Sons Ltd, July 2012.

[3] S. Jose, "Cisco visual networking index: Forecast and trends, 2017–2022," 2018.

[4] Federal Communications Commission (FCC), "Spectrum Policy Task Force," ET Docket no. 02-135, Nov. 15, 2002.

[5] S. Geirhofer, L. Tong, and B. M. Sadler, "Cognitive medium access: Constraining interference based on experimental models," *IEEE Journal on Selected Areas in Communications*, vol. 26, no. 1, pp. 95–105, Jan. 2008.

[6] J. Mitola, "Cognitive radio for flexible mobile multimedia communications," in *IEEE International Workshop on Mobile Multimedia Communications*, 1999, pp. 435–441.

[7] R. Tandra, S. M. Mishra, and A. Sahai, "What is a spectrum hole and what does it take to recognize one?" *Proceedings of the IEEE*, vol. 97, no. 5, pp. 824–848, Apr. 2009.

[8] H. Shiang and M. van der Schaar, "Queuing-based dynamic channel selection for heterogeneous multimedia applications over cognitive radio networks," *IEEE Transactions on Multimedia*, vol. 10, no. 5, pp. 896–909, Aug. 2008.

[9] M. Song, C. Xin, Y. Zhao, and X. Cheng, "Dynamic spectrum access: from cognitive radio to network radio," *IEEE Wireless Communications*, vol. 19, no. 1, pp. 23–29, Feb. 2012.

[10] S. Mao and D. Hu, "Video over cognitive radio networks: When compression meets the radios," *E-Letter of the Multimedia Communications Technical Committee*, vol. 5, no. 6, Nov. 2010.

[11] F. F. Digham, M.-S. Alouini, and M. K. Simon, "On the energy detection of unknown signals over fading channels," *IEEE Transactions on Communications*, vol. 55, no. 1, pp. 21–24, May 2007.

[12] R. Tandra and A. Sahai, "SNR walls for signal detection," *IEEE Journal of Selected Topics in Signal Processing*, vol. 2, no. 1, pp. 4–17, Feb. 2008.

[13] A. Sahai, N. Hoven, and R. Tandra, "Some fundamental limits on cognitive radio," in *Allerton Conference on Communication, Control, and Computing*, Monticello, Illinois, 2004, pp. 1662–1671.

[14] D. Cabric, S. M. Mishra, and R. W. Brodersen, "Implementation issues in spectrum sensing for cognitive radios," in *Thirty-Eighth Asilomar Conference on Signals, Systems and Computers*, vol. 1, 2004, pp. 772–776.

[15] A. Fehske, J. Gaeddert, and J. H. Reed, "A new approach to signal classification using spectral correlation and neural networks," in *First IEEE International Symposium on New Frontiers in Dynamic Spectrum Access Networks*, 2005, pp. 144–150.

[16] S. Haykin, D. J. Thomson, and J. H. Reed, "Spectrum sensing for cognitive radio," *Proceedings of the IEEE*, vol. 97, no. 5, pp. 849–877, Apr. 2009.

[17] P. D. Sutton, K. E. Nolan, and L. E. Doyle, "Cyclostationary signatures in practical cognitive radio applications," *IEEE Journal on Selected Areas in Communications*, vol. 26, no. 1, pp. 13–24, 2008.

[18] Y. Zeng and Y.-C. Liang, "Eigenvalue-based spectrum sensing algorithms for cognitive radio," *IEEE Transactions on Communications*, vol. 57, no. 6, pp. 1784–1793, Jun. 2009.

[19] Y. Zeng and Y. Liang, "Maximum-minimum eigenvalue detection for cognitive radio," in *IEEE 18th International Symposium on Personal, Indoor and Mobile Radio Communications*, Sep. 2007, pp. 1–5.

[20] K. Pelechrinis, P. Krishnamurthy, M. Weiss, and T. Znati, "Cognitive radio networks: realistic or not?" *ACM SIGCOMM Computer Communication Review*, vol. 43, no. 2, pp. 44–51, 2013.

[21] E. Z. Tragos, S. Zeadally, A. G. Fragkiadakis, and V. A. Siris, "Spectrum assignment in cognitive radio networks: A comprehensive survey," *IEEE Communications Surveys & Tutorials*, vol. 15, no. 3, pp. 1108–1135, Jan. 2013.

[22] H. G. Sandalidis and P. Stavroulakis, "Heuristics for solving fixed-channel assignment problems," in *Handbook of Wireless Networks and Mobile Computing*, I. Stojmenovic, Ed., John Wiley & Sons, Inc. Wiley Online Library, February 2002, pp. 51–77.

[23] D. H. Lee, W. S. Jeon, and D. G. Jeong, "Joint channel assignment and routing in cognitive radio-based wireless mesh networks," in *IEEE 71st Vehicular Technology Conference*, 2010, pp. 1–5.

[24] M. Bkassiny and S. K. Jayaweera, "Optimal channel and power allocation for secondary users in cooperative cognitive radio networks," in *International Conference on Mobile Lightweight Wireless Systems*, 2010, pp. 180–191.

[25] Q. Xin and J. Xiang, "Joint qos-aware admission control, channel assignment, and power allocation for cognitive radio cellular networks," in *IEEE 6th International Conference on Mobile Adhoc and Sensor Systems*, 2009, pp. 294–303.

[26] H. B. Salameh, M. Krunz, and O. Younis, “Distance-and traffic-aware channel assignment in cognitive radio networks,” in *5th Annual IEEE Communications Society Conference on Sensor, Mesh and Ad Hoc Communications and Networks*, 2008, pp. 10–18.

[27] E. A. Silver, “An overview of heuristic solution methods,” *Journal of the Operational Research Society*, vol. 55, no. 9, pp. 936–956, Sep. 2004.

[28] N. Nie, C. Comaniciu, and P. Agrawal, “A game theoretic approach to interference management in cognitive networks,” in *Wireless Communications*, 2007, pp. 199–219.

[29] N. Nie and C. Comaniciu, “Adaptive channel allocation spectrum etiquette for cognitive radio networks,” *Mobile Networks and Applications*, vol. 11, no. 6, pp. 779–797, 2006.

[30] H. Zhang and X. Yan, “Advanced dynamic spectrum allocation algorithm based on potential game for cognitive radio,” in *IEEE 2nd International Symposium on Information Engineering and Electronic Commerce*, 2010, pp. 1–3.

[31] G. Liu, L. Zhou, K. Xiao, B. Yu, G. Zhou, B. Wang, and X. Zhu, “Receiver-centric channel assignment model and algorithm in cognitive radio network,” in *IEEE 4th International Conference on Wireless Communications, Networking and Mobile Computing*, 2008, pp. 1–4.

[32] I. Malanchini, M. Cesana, and N. Gatti, “On spectrum selection games in cognitive radio networks,” in *Global Telecommunications Conference*, 2009, pp. 1–7.

[33] H. Wang, J. Ren, and T. Li, “Resource allocation with load balancing for cognitive radio networks,” in *Global Telecommunications Conference*, 2010, pp. 1–5.

[34] A. T. Hoang and Y.-C. Liang, “Downlink channel assignment and power control for cognitive radio networks,” *IEEE Transactions on Wireless Communications*, vol. 7, no. 8, pp. 3106–3117, 2008.

[35] L. Yu, C. Liu, and W. Hu, “Spectrum allocation algorithm in cognitive ad-hoc networks with high energy efficiency,” in *International Conference on Green Circuits and Systems*, 2010, pp. 349–354.

[36] P. Kaur, M. Uddin, and A. Khosla, “Adaptive bandwidth allocation scheme for cognitive radios.” *International Journal of Advancements in Computing Technology*, vol. 2, no. 2, pp. 35–41, 2010.

[37] Z. Wenzhu and L. Xuchen, “Centralized dynamic spectrum allocation in cognitive radio networks based on fuzzy logic and q-learning,” *China Communications*, vol. 8, no. 7, pp. 46–54, 2011.

[38] F. Ye, R. Yang, and Y. Li, “Genetic spectrum assignment model with constraints in cognitive radio networks,” *International Journal of Computer Network and Information Security*, vol. 3, no. 4, pp. 39–45, 2011.

[39] Z. Zhao, Z. Peng, S. Zheng, and J. Shang, "Cognitive radio spectrum allocation using evolutionary algorithms," *IEEE Transactions on Wireless Communications*, vol. 8, no. 9, pp. 4421–4425, 2009.

[40] F. Ye, R. Yang, and Y. Li, "Genetic algorithm based spectrum assignment model in cognitive radio networks," in *2nd International Conference on Information Engineering and Computer Science*, 2010, pp. 1–4.

[41] M. Y. ElNainay, F. Ge, Y. Wang, A. E. Hilal, Y. Shi, A. B. MacKenzie, and C. W. Bostian, "Channel allocation for dynamic spectrum access cognitive networks using localized island genetic algorithm," in *5th International Conference on Testbeds and Research Infrastructures for the Development of Networks & Communities and Workshops*, 2009, pp. 1–3.

[42] M. Y. El Nainay, D. H. Friend, and A. B. MacKenzie, "Channel allocation & power control for dynamic spectrum cognitive networks using a localized island genetic algorithm," in *3rd IEEE Symposium on New Frontiers in Dynamic Spectrum Access Networks*, 2008, pp. 1–5.

[43] L. Liu, G. Hu, and Y. Peng, "Swarm intelligence based distributed spectrum allocation for cognitive networks," in *International Conference on Future Information Technology*, vol. 13, 2011, pp. 357–361.

[44] X. Cheng and M. Jiang, "Cognitive radio spectrum assignment based on artificial bee colony algorithm," in *IEEE 13th International Conference on Communication Technology*, 2011, pp. 161–164.

[45] M. Sauter, *From GSM to LTE: an introduction to mobile networks and mobile broadband*. Third Avenue, NY: John Wiley & Sons Ltd, July 2014.

[46] H. A. M. Ramli, K. Sandrasegaran, R. Basukala, R. Patachaianand, M. Xue, and C.-C. Lin, "Resource allocation technique for video streaming applications in the lte system," in *The 19th Annual Wireless and Optical Communications Conference*, 2010, pp. 1–5.

[47] M. Hassan and M. Krunz, "Video streaming over wireless packet networks: An occupancy-based rate adaptation perspective," *IEEE Transactions on Circuits and Systems for Video Technology*, vol. 17, no. 8, pp. 1017–1027, 2007.

[48] H. Schwarz, D. Marpe, and T. Wiegand, "Overview of the scalable video coding extension of the H. 264/AVC standard," *IEEE Transactions on Circuits and Systems for Video Technology*, vol. 17, no. 9, pp. 1103–1120, 2007.

[49] H. Hellwagner, I. Kofler, M. Eberhard, R. Kuschnig, M. Ransburg, and M. Sablatschan, "Scalable video coding: Techniques and applications for adaptive streaming," in *IGI Global*, 2011, pp. 1–23.

[50] S. Khan, Y. Peng, E. Steinbach, M. Sgroi, and W. Kellerer, "Application-driven cross-layer optimization for video streaming over wireless networks," *IEEE Communications Magazine*, vol. 44, no. 1, pp. 122–130, 2006.

[51] A. E. Omer, M. S. Hassan, and M. El-Tarhuni, "An integrated scheme for streaming scalable encoded video-on-demand over CR networks," *Physical Communication*, vol. 35, pp. 1–11, 2019.

[52] A. E. Omer, M. Hassan, and M. El-Tarhuni, "A joint adaptive approach for on-demand scalable video streaming over CR networks," in *2016 European Modelling Symposium (EMS)*. IEEE, 2016, pp. 186–191.

[53] A. E. Omer, M. S. Hassan, and M. El-Tarhuni, "Window-based adaptive technique for real-time streaming of scalable video over cognitive radio networks," *IET Communications*, vol. 11, no. 17, pp. 2643–2649, 2017.

[54] O. Sweileh, M. S. Hassan, H. S. Mir, and M. H. Ismail, "A switching-based and delay-aware scheduling algorithm for cognitive radio networks," *International Journal of Interdisciplinary Telecommunications and Networking (IJITN)*, vol. 11, no. 3, pp. 34–48, 2019.

[55] Y. A. Rahama, M. S. Hassan, and M. H. Ismail, "A stochastic-based rate control approach for video streaming over cognitive radio networks," *IEEE Transactions on Cognitive Communications and Networking*, vol. 5, no. 1, pp. 181–192, 2018.

[56] S. Dey and I. S. Misra, "Content driven proportionate channel allocation scheme for scalable video over cognitive radio network," in *IEEE Calcutta Conference*, 2020, pp. 59–63.

[57] H. B. Salameh and R. Abusamra, "Intelligent multicast routing for multimedia over cognitive radio networks: a probabilistic approach," *Multimedia Tools and Applications*, vol. 1, no. 1, pp. 1–12, 2020.

[58] A. Ali, S. Tariq, M. Iqbal, L. Feng, I. Raza, M. H. Siddiqi, and A. K. Bashir, "Adaptive bitrate video transmission over cognitive radio networks using cross layer routing approach," *IEEE Transactions on Cognitive Communications and Networking*, vol. 1, pp. 121–130, April 2020.

[59] A. Ali, M. E. Ahmed, F. Ali, N. H. Tran, D. Niyato, and S. Pack, "Non-parametric bayesian channels clustering (NOBEL) scheme for wireless multimedia cognitive radio networks," *IEEE Journal on Selected Areas in Communications*, vol. 37, no. 10, pp. 2293–2305, 2019.

[60] S.-Y. Lien, K.-C. Chen, Y.-C. Liang, and Y. Lin, "Cognitive radio resource management for future cellular networks," *IEEE Wireless Communications*, vol. 21, no. 1, pp. 70–79, 2014.

[61] S. Sesia, I. Toufik, and M. Baker, *LTE-the UMTS long term evolution: from theory to practice*. John Wiley & Sons, 2011.

[62] "Physical layer procedures, 3GPP TS 36.213," 3GPP TR Release 13, 2016. [Online]. Available: https://www.etsi.org/deliver/etsi_ts/136200_136299/136213/13.00.00_60/ts_136213v130000p.pdf [Accessed: Jan. 16, 2019].

[63] A. Asheralieva and K. Mahata, “Resource allocation for lte-based cognitive radio network with queue stability and interference constraints,” *Physical Communication*, vol. 14, pp. 1–13, 2015.

[64] B. Kouassi, L. Deneire, B. Zayen, R. Knopp, F. Kaltenberger, F. Negro, D. Slock, and I. Ghaur, “Design and implementation of spatial interweave lte-tdd cognitive radio communication on an experimental platform,” *IEEE Wireless Communications*, vol. 20, no. 2, pp. 60–67, 2013.

[65] J. D. Naranjo, I. Viering, and K.-J. Friederichs, “A cognitive radio based dynamic spectrum access scheme for lte heterogeneous networks,” in *IEEE Wireless Telecommunications Symposium*, 2012, pp. 1–7.

[66] S. N. Shankar, C.-T. Chou, K. Challapali, and S. Mangold, “Spectrum agile radio: capacity and QOS implications of dynamic spectrum assignment,” in *IEEE Global Telecommunications Conference*, vol. 5, no. 7, Nov. 2005, pp. 2510–2516.

[67] M. Derakhshani and T. Le-Ngoc, “Learning-based opportunistic spectrum access with adaptive hopping transmission strategy,” *IEEE Transactions on Wireless Communications*, vol. 11, no. 11, pp. 3957–3967, Nov. 2012.

[68] S. Bayhan and F. Alagöz, “A markovian approach for best-fit channel selection in cognitive radio networks,” *Ad Hoc Networks*, vol. 12, no. 11, pp. 165–177, 2014.

[69] Y. Saleem and M. H. Rehmani, “Primary radio user activity models for cognitive radio networks: A survey,” *Journal of Network and Computer Applications*, vol. 43, no. 1, pp. 1–16, 2014.

[70] W. Lee and I. F. Akyildiz, “Optimal spectrum sensing framework for cognitive radio networks,” *IEEE Transactions on Wireless Communications*, vol. 7, no. 10, pp. 3845–3857, Oct. 2008.

[71] Y. Chen, Q. Zhao, and A. Swami, “Joint design and separation principle for opportunistic spectrum access in the presence of sensing errors,” *IEEE Transactions on Information Theory*, vol. 54, no. 5, pp. 2053–2071, May 2008.

[72] A. A. Daoud, M. Alanyali, and D. Starobinski, “Secondary pricing of spectrum in cellular CDMA networks,” in *2nd IEEE International Symposium on New Frontiers in Dynamic Spectrum Access Networks*, 2007, pp. 535–542.

[73] C. Chou, S. S. N, H. Kim, and K. G. Shin, “What and how much to gain by spectrum agility?” *IEEE Journal on Selected Areas in Communications*, vol. 25, no. 3, pp. 576–588, Apr. 2007.

[74] B. Canberk, I. F. Akyildiz, and S. Oktug, “Primary user activity modeling using first-difference filter clustering and correlation in cognitive radio networks,” *IEEE/ACM Transactions on Networking*, vol. 19, no. 1, pp. 170–183, Feb. 2011.

[75] M. Khabazian, S. Aissa, and N. Tadayon, “Performance modeling of a two-tier primary-secondary network operated with IEEE 802.11 DCF mechanism,” *IEEE*

Transactions on Wireless Communications, vol. 11, no. 9, pp. 3047–3057, Sep. 2012.

[76] Y. A. Rahama, M. S. Hassan, and M. H. Ismail, "A novel closed-form expression for the probability of starvation in video streaming over wireless networks," *Telecommunication Systems*, vol. 71, no. 4, pp. 577–584, 2019.

[77] R. L. Batista, C. F. M. e Silva, T. F. Maciel, J. M. B. da Silva, and F. R. Cavalcanti, "Joint opportunistic scheduling of cellular and device-to-device communications," *Journal of Communication and Information Systems*, vol. 32, no. 1, pp. 62–73, 2017.

[78] F. Li, P. Ren, and Q. Du, "Joint packet scheduling and subcarrier assignment for video communications over downlink ofdma systems," *IEEE Transactions on Vehicular Technology*, vol. 61, no. 6, pp. 2753–2767, 2012.

[79] Y. Zhang and G. Liu, "Fine granularity resource allocation algorithm for video transmission in orthogonal frequency division multiple access system," *IET Communications*, vol. 7, no. 13, pp. 1383–1393, 2013.

[80] H. Xing and S. Hakola, "The investigation of power control schemes for a device-to-device communication integrated into ofdma cellular system," in *21st Annual IEEE International Symposium on Personal, Indoor and Mobile Radio Communications*, 2010, pp. 1775–1780.

[81] Y.-W. Kuo and L.-D. Chou, "Power saving scheduling scheme for internet of things over lte/lte-advanced networks," *Mobile Information Systems*, vol. 1, pp. 1–11, 2015.

Appendix

In this section, we present tables used in rate calculation in section 4.3. Table 1 maps modulation order index to the TBS index ITBS. SUs report the measured CQI to the BS by mapping the measured SNR according to Table 2. The transport block size is found using the number of RBs assigned to the SU and TBS index I_{TBS} based on Table 3, that reveals part of the Transport block size table provided by LTE specifications.

Table 1: Modulation and TBS index table

I_{MCS}	Modulation	I_{TBS}
0	2	0
1	2	1
2	2	2
3	2	3
4	2	4
5	2	5
6	2	6
7	2	7
8	2	8
9	2	9
10	4	9
11	4	10
12	4	11
13	4	12
14	4	13
15	4	14
16	4	15
17	6	15
18	6	16
19	6	17
20	6	18
21	6	19
22	6	20
23	6	21
24	6	22
25	6	23
26	6	24
27	6	25
28	6	26

Table 2: SNR to CQI mapping and I_{MCS}

CQI	SNR	Modulation	I_{MCS}
1	-6.7	QPSK	0
2	-4.7	QPSK	0
3	-2.3	QPSK	2
4	0.2	QPSK	5
5	2.4	QPSK	7
6	4.3	QPSK	9
7	5.9	16-QAM	12
8	8.1	16-QAM	14
9	10.3	16-QAM	16
10	11.7	64-QAM	20
11	14.1	64-QAM	23
12	16.3	64-QAM	25
13	18.7	64-QAM	27
14	21	64-QAM	28
15	22.7	64-QAM	28

Table 3: Transport block size table.

I_{TBS}	N_{PRB}									
	1	2	3	4	5	6	7	8	9	10
0	16	32	56	88	120	152	176	208	224	256
1	24	56	88	144	176	208	224	256	328	344
2	32	72	144	176	208	256	296	328	376	424
3	40	104	176	208	256	328	392	440	504	568
4	56	120	208	256	328	408	488	552	632	696
5	72	144	224	328	424	504	600	680	776	872
6	328	176	256	392	504	600	712	808	936	1032
7	104	224	328	472	584	712	840	968	1096	1224
8	120	256	392	536	680	808	968	1096	1256	1384
9	136	296	456	616	776	936	1096	1256	1416	1544
10	144	328	504	680	872	1032	1224	1384	1544	1736

Vita

Maram Wahed Rashad Helmy was born in 1993, in Alexandria, in Egypt. She received her primary and secondary education in Ras Al Khaimah, UAE, and graduated from Al Kharan high school in 2011 with an average of (97%). In 2016, she graduated from the American University of Ras Al Khaimah with a Bachelor's degree in Electronics and Communication Engineering with the highest honor Summa cum laude and GPA of (3.97/4.0). In 2017, she worked as a research assistant at American University of Ras Al Khaimah and co-authored four publications; three conference papers and one journal. In 2018, she joined Electrical Engineering Master's program at the American University of Sharjah, where she was granted a graduate teaching assistantship. She co-authored one paper during her Master's study which was presented in WTS conference on April 9, 2019.

Her research interests are in multimedia streaming, wireless communications, digital signal processing and machine learning.